CICIND

Commentaries for the

Model Code for Concrete Chimneys

Part A: The Shell

Second Edition, Revision 1

August 2001

ISBN 1-902998-14-6

Office of The Secretary
CICIND, 14 The Chestnuts, Beechwood Park, Hemel Hempstead, Herts. HP3 0DZ, UK
Tel: +44(0)1442211204 Fax: +44(0)1442256155 e-mail: secretary@cicind.org

www.cicind.org

Contents

Introduction

These Commentaries are largely derived from those published in April 1987 to accompany the first edition of the "Model Code for Concrete Chimneys - Part A: The Shell" which was published in October 1984. They have been enlarged and updated to reflect the changes in the Second Edition of the Code first published in August 1998 and subsequently revised and reprinted in loose-leaf format in August 2001. Advantage has been taken of the opportunity to include recommendations for Capacity Design in the section on Seismic actions.

CICIND, Zurich, Switzerland

- Office of the Secretary -

CICIND, 14 The Chestnuts, Beechwood Park, Hemel Hempstead HP3 0DZ, England.

Commentary No. 1

Failure Probability and Safety Factors

Table of Contents

1 Introduction

The choice of load factors depends on the risk of failure that is considered acceptable. Consequently this commentary falls naturally into two parts:

1. Choice of appropriate failure probability.
2. Estimation of the partial safety factors required to achieve the specified probability.

2 Justification of the target failure probability

The acceptable level of risk of failure should be assessed with regard to two criteria:

Social - the risk to human life as a consequence of collapse,

Economic - the consequential cost of failure or unserviceability.

2.1 Social criteria

CIRIA Report 63[1] published in 1977 gives the following formula for calculating the acceptable total lifetime risk:

$$P_{ft} = \frac{10^{-4}}{n_r} K_s n_d \qquad (1)$$

in which

n_r is the average number of people in or near the structure during the period of risk
K_s is a social criterion factor, given in Table 1 for various types of structure
P_{ft} is the target probability of failure of the structure due to any cause in its design life
n_d is the design life of the structure in years

For an industrial chimney the types of failure which could endanger life are collapse of the shell or flue **support structure.**

Table 1 Social criterion factors

Nature of structure	K_s
Places of public assembly, dams	0.005
Domestic, office or trade and industry	0.05
Bridges	0.5
Towers, masts, offshore structures	5.0

In order to use equation 1 it is necessary to estimate n_r. It is suggested [1,2] that allowance be made for the degree of correlation between the loading leading to failure and the number of people likely to be close to or on the structure. Since collapse is most likely to occur under extreme wind speeds, it may be assumed that nobody will be in or near the chimney except through necessity. Thus the value of n_r may be assumed to lie in the range 0.1 to 10 with due regard to the average periods of occupation of the vulnerable buildings, their proximity and the direction of the prevailing wind.

Assuming that $n_d = 50$ and $K_s = 0.05$ gives the values of P_f in Table 2

Table 2 Typical failure probabilities P_f for environmental risk

Environment	number of fatalities	Pf
small steel chimney in industrial area	0.1	2-5-10-3
large power station or oil refinery chimney	1	$2.5.10^{-4}$
large CHP in urban area or hospital chimney	10	$2.5.10^{-5}$

2.2 Economic criteria

Another consideration is the balance between initial cost and the economic consequences of failure. The approach requires several assumptions, such as the cost of finance, the rate of inflation and the relation between the cost of construction and the partial safety factors. Figure 1 shows a typical family of curves relating the total cost to the failure probability p for various ratios g of total cost to initial cost. Ideally the failure probability should be chosen to minimise the total cost. Because of the uncertainties inherent in the assumptions these curves are not to be taken literally, but they do indicate that a target of 10^{-4} for the lifetime failure probability of most concrete chimneys is reasonable, and that it would be unwise to increase it in view of the steep rise in total cost in the direction of decreasing load factor. For 'normal' structures, CEN[3] recommends a 'reliability index' of 3.8, corresponding to a lifetime failure probability of 7.10^{-5}, which is close enough.

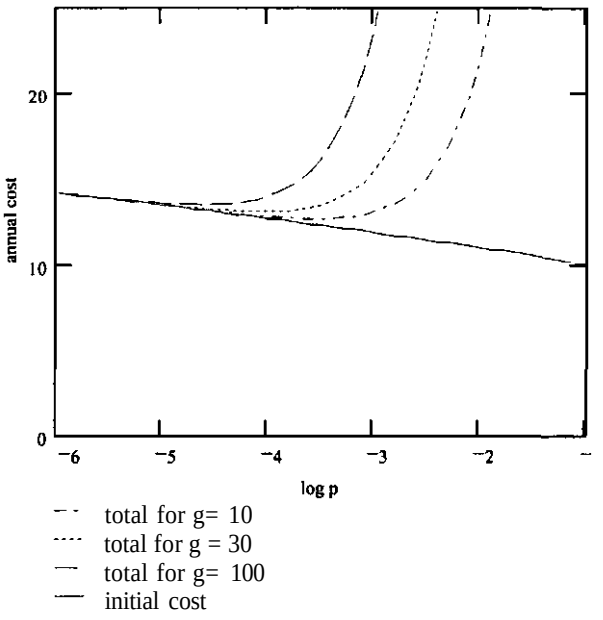

Fig.1 Total Cost vs. Failure Probability

2.3 Importance classes

If the chimney is of great economic importance, for example the sole multiflue chimney serving a 4GW power station, the consequential cost of failure may be so great that the total cost of collapse approaches 100 times the initial cost. In this case the target probability should be reduced to 10^{-5}. For this reason CICIND distinguishes between two Importance Classes as described in Table 3.

Table 3: Importance Classes for Concrete Chimneys

Class	Description	Target P_f
1	normal chimneys	10^{-4}
2	chimneys of exceptional economic or social importance	10^{-5}

It is suggested that the importance class be specified by the owner.

3 Choice of partial safety factors for the ultimate limit state

3.1 Definition of Failure

A chimney cross-section fails if the external forces M_w and N_p due to actions such as wind and permanent load are outside the range of those values M_u and N_u which the cross-section can withstand. Neither pair of values is known exactly. At best their probability distributions can be estimated:

- M_w and N_p depend on the probabilistic behaviour of the actions.
- M_u and N_u depend on the probabilistic behaviour of the properties of the materials and of the dimensions.

The probability of failure is controlled by the partial safety factors. It will be shown that the factors given below lead to the required probabilities for the ultimate limit state of failure due to inline wind.

Concrete	γ_{cu}	= 1.5
reinforcement	γ_{su}	= 1.15
permanent load	γ_{Pu}	= 1.0
inline wind, class 1	γ_{Wu}	= 1.6
inline wind, class 2	γ_{Wu}	= 1.8

3.2 Method for the determination of the failure probability

The principles involved are described in detail in the literature [4],[5]. For this commentary the method used is based on the multivariate analysis of the 1986 edition of this Commentary with the exception of the probability distribution for wind.

For the determination of the failure probability of a chimney cross-section, many random variables are required. For the purpose of this commentary the six variables of Table 4 have been selected as random variables whereas other influencing factors, such as ratio of reinforcement p and shell diameter d, have been treated as deterministic values since their deviation is very small. For the calculation normalised values from Table 4 are used.

Table 4: Random Variables for the determination of the failure probability of chimney cross-sections

	Influence	Random Values	Characteristic Values	Normalised Values	Distribution	Parameters
1	Concrete strength	f_c	f_{ck}	$k_c = f_c/f_{ck}$	log-normal	mean f= 38.0 MPa s.d. S_c =4.9 MPa
2	Steel strength	fs	f_{sk}	$k_s = f_s/f_{sk}$	log-normal	mean f_{sm} =450 MPa s.d. S_s = 30.4 MPa
3	Wall thickness	t	t_k	$k_t = t/t_k$	normal	mean k_{tm} =1 .00 s.d. S_t = 0.03
4	Model factor	Mod	Mod_k	$K_{MO} = Mod/Mod_k$	normal	mean k_{mod} = 0.90 s.d. S_{mod} =0.061
5	Normal force	N	N_k	$k_N = N/N_k$	normal	mean k_{Nm} = 1 .00 s.d. S_N = 0.043
6	Bending moment from wind	M	M_k	$k_M = M/M_k$	FT1 for pressure (v^2)	mode u_{Mm} = 400 dispersion $1/a_M$ = 80

The following normalised cross-sectional forces are used in the calculations:

- random values

$$n = \frac{N \cdot Mod}{\pi \cdot d \cdot t \cdot f_c} \tag{2}$$

$$m = \frac{M \cdot Mod}{\pi \cdot d^2 \cdot t \cdot f_c} \tag{3}$$

- characteristic values

$$n_k = \frac{N_k \cdot Mod_k}{\pi \cdot d \cdot t_k \cdot f_{ck}} \tag{4}$$

$$m_k = \frac{M_k \cdot Mod_k}{\pi \cdot d^2 \cdot t \cdot f_{ck}} \tag{5}$$

The failure probability P_F is given by equation 6

$$P_F = \int_0^\infty \int_0^\infty \int_0^\infty \int_0^\infty \int_0^\infty \int_0^\infty p_c\, p_s\, p_t\, p_{Mo}\, p_N\, p_M \cdot c_u \cdot df_c\, df_s\, dt\, dMo\, dN\, dM \tag{6}$$

The "failure factor" c_u which appears In this integral is determined as follows:

For each combination of f_c, f_s, t, Mod, N, and M the strains are determined for the condition of equilibrium.

If one of the strains at the edge of the cross-section exceeds the ultimate limit strain the factor c_u =1: otherwise c_u = 0.

The determination of c_u is the real task of the evaluation of the integral.

The integral (6) was evaluated by two independent methods:

1. As in the 1987 edition of this commentary, but with an increased number of intervals.
2. By a Monte Carlo method using a variety of pseudo-random number generators to calculate values of the variables.

The results obtained by the two methods were in close agreement[5].

3.3 Calculation of the Failure Factor c_u

Each combination of the parameters f_c, f_s, k_t, k_N and k_{Mo} gives a normalised failure moment m_u which the chimney can withstand. This moment is determined as follows:

The normalised ultimate normal force is calculated using the relation

$$n_u = \frac{n_k \cdot k_N}{k_t \cdot k_c} \tag{7}$$

The corresponding normalised ultimate bending moment m_u is calculated as a function of n_u, f_c and f_s.

The random bending moment due to wind is calculated from the wind velocity by:

$$m_w = \frac{m_k \cdot k_{Mo}}{k_t \cdot k_c} \left(\frac{v}{v_k} \right)^2 \tag{8}$$

Using the values of m_u and m_w the failure factor c_u is determined from:

$$\begin{aligned} c_u &= 1 \quad \text{for} \quad m_w \geq m_u \\ c_u &= 0 \quad \text{for} \quad m_w < m_u \end{aligned} \tag{9}$$

If the density distributions of the single parameters are known, the failure probability of chimney cross-sections can now be determined according to equation (6).

3.4 Assumptions for the extreme-value distribution for wind

The distribution of extreme values of wind velocity is not Gaussian [6],[7]. We take the Gumbel formula for the cumulative probability of wind pressure, which leads to the following expression for the cumulative probability as a function of the velocity.

$$P_1(v) = \exp(-\exp(-a(v^2 - u)) \quad (10)$$

Following [7], we assume that the product a.u = 5, which is recommended for the wind climate of the UK and may be regarded as typical for many other regions. Larger values of the product lead to lower predicted failure probabilities and vice versa.

The characteristic wind velocity according to the Model Code is defined as the wind speed with a probability of being exceeded of 0.02 in one year (50 year return period). As the design life is 50 years, the 50-year wind distribution P_{50} (v) must be used in the calculation of failure probability. This is derived from P_1(v) by the equation

$$P_{50}(v) = (P_1(v))^{50} \quad (11)$$

4 Results and Justification of the CICIND Safety Factors

4.1 Inline wind - final state

The integral (6) has been evaluated for a series of values of the normalised force n_k. The corresponding normalised moment m_k is computed from n_k on the basis of the CICIND Model Code. These two values n_k and m_k then uniquely determine all the values needed for the integration. The result is shown in Table 5, which shows that in the relevant range of eccentricities the values of failure probability are in the region of 10_{-4}forγ_w =1.6 and 10^{-5}forγ_w = 1.8. This is the justification of the CICIND safety factors for the inline wind load case.

Table 5: Failure probabilities for the chimney cross-section

n_u	0	0.05	0.10	0.15	0.20	0.25	0.30
m_u	0.026	0.049	0.069	0.087	0.099	0.106	0.105
$P \cdot 10^6$ (γ_w = 1.6)	34	117	163	101	34	7	1
$P \cdot 10^6$ (γ_w = 1.8)	2	11	17	9	2	0	0

4.2 Safety Factor for Earthquake

A similar analysis of the earthquake load case is not possible because the frequency distribution of the extreme values is not known with sufficient accuracy.

It is considered that the proposed safety factor γ_{Eu} = 1.4 is sufficient.

This value is related to the greatest earthquake which can be expected in the light of past observations.

4.3 Safety Factor for the Construction State

In the First Edition of this Code the construction state was given a separate wind load factor. In the Second Edition this has been replaced by the CEN recommendation [7] to reduce the inline wind load to 80% of its 50-year value on account of the reduced period of exposure.

4.4 Safety Factor for Corbel Loading

The safety factor of γ_{Pu} = 1.4 was adopted because of the great importance of corbels.

4.5 Safety Factor for the Serviceability Limit State

Interior installations must be able to stand the deflection of the shell without loss of serviceability.

A safety factor of γ_{Ws} = 1.3 is recommended.

5 Summary

A multivariate analysis has been used to determine the failure probabilities of chimney cross-sections. The random parameters are as follows:

- strength of concrete
- strength of steel
- wall thickness
- modelling factor (degree of accordance between the calculation model and the real structure)
- normal force
- wind moment

Reasonable probability distributions have been chosen for these parameters.

The CICIND safety factors result in lifetime failure probabilities of around 10^{-4} for normal (class 1) chimneys and 10^{-5} for exceptionally important (class 2) chimneys.

List of Literature

1. Construction Industry Research and Information Association: "Rationalisation of safety and serviceability factors in structural codes" (CIRIA Report 63), July 1977
2. Pinfold.G.M.: "Tall Concrete Stacks: Cost Sensitivity and Optimisation" , Proc. 2nd International Chimney Symposium, Edinburgh 1976
3. CEN: ENV 1991-1,1994
4. Bottenbruch, H., Noakowski, P.: "Versagenswahrscheinlichkeit von turmartigen Bauwerken nach der direkten Integrationsmethode unter Zugrundelegung von verschiedenen Normen"; Bauingenieur 62 (1987), pages 29-40.
5. Bierrum, N.R.: "Failure Probability and Load Factors", CICIND Report Vol.14 No.1, CICIND May 1998.
6. Cook, N.J.: "Towards Better Estimation of Extreme Winds" J. Wind Eng. Ind. Aerodyn. 9(1982).
7. CEN: ENV 1991-2-4,1997.

Commentary No. 2

Material Law in the Ultimate Limit State

Table of Contents

1 Introduction

The following forces act on the horizontal cross-sections of a chimney:

- permanent global normal forces N from dead load
- short-term global bending moments M from wind
- long-term local bending moments ΔM from temperature differences and from corbel loading.

The effect of repeated loads due to oscillation is of little significance in concrete chimneys [3] and has not been taken into account.

Generally, these three load cases appear together. The behaviour of the reinforced concrete, however, varies considerably when the two limiting load cases are considered:

- permanent loading from dead load alone
  N from dead load, M = 0, e = M/N = 0

and

- a short-term transient from wind load alone
  N = 0, M from wind, e = M/N = ∞

CEN [1] considers for all load cases the behaviour of the concrete under permanent loading only. The 1984 edition of the CICIND Model Code took into account the effect of duration of the load on concrete behaviour.

2 Ultimate Limit State of Concrete

The 1984 edition was based on a material law which assumed the concrete stress-strain relationship to be parabolic under long-term loading and linear under short-term loading. Consequently the concrete strain at failure was limited to about 0.001. The effect on the design strength can be seen in Figures 1 and 2, which have been calculated with the same material factors for both old and new laws.

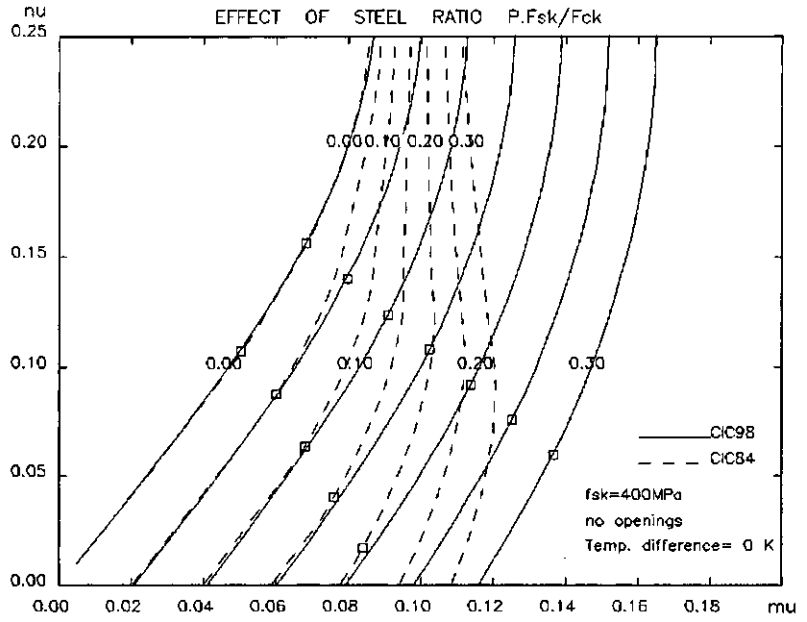

Fig. 1 - Comparison of design strengths for the old and new material laws - no openings

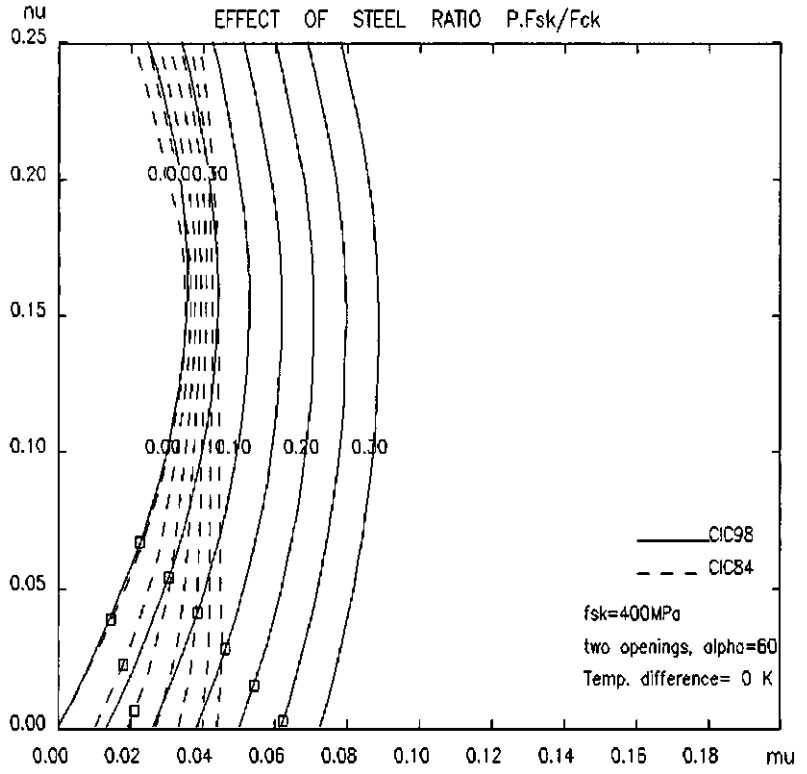

Fig.2 - Comparison of design strengths for the old and new material laws - two opposed openings

In these diagrams the balance points, at which both reinforcement and concrete strains reach their limiting values, are marked by small squares. Up to the balance points the two laws give similar results; beyond them the behaviour is very different.

This change in the predicted behaviour requires justification. Accordingly the calculation method of Commentary 1 was applied to this problem. The CEN stress-strain law was assumed with restrictions on the maximum strain but ignoring other short-term effects. To summarise the results:-

1. Reducing the material factor for concrete from 1.5 to 1.2 has little effect on the highest failure rate in the range considered. This is because the large factor makes concrete failure extremely unlikely.
2. Reducing the maximum concrete strain to 0.0018 also has little effect on the highest failure rate.

The main reason for the difference in the ultimate moments predicted by the two laws is that under the 1984 law the tensile reinforcement is far from fully utilised when the concrete strain reaches the limiting value.

The conclusion is that the material law of the 1984 code represents an unwarranted oversimplification of the actual short-term behaviour of concrete.

3 Ultimate Limit State of Reinforcement

The behaviour of steel reinforcement does not depend on short-term or long-term load in the periods of oscillation which are valid for chimneys. This justifies the idealised material law given in section 6.2.6 of the Model Code.

The ultimate limit strain ε_{su} = 0.01 usually applied in reinforced concrete constructions can be used for chimneys since it was proved in [3] that the fracture is not caused by repeated oscillation loading due to wind but by a single wind gust.

List of Literature

1. Comite Euro-International du Beton: CEB/FIP international Recommendations for the Design and Construction of Concrete Structures. Principles and Recommendations.", 1978
2. Deutsches Institut für Normung: DIN 1056, "Solid Construction, Freestanding Stacks; Calculation and Design", October 1984.
3. Schueller, G.I. & Bucher C.G.: "On the Failure Mechanisms of Reinforced Concrete Chimneys"; CICIND Report vol.13no.2,September 1997.
4. Grasser, E.: "Darstellung und kritische Analyse der Grundlagen für eine wirklichkeitsnahe Bemessung von Stahlbetonquerschnitten bei einachsigen Spannungszustanden", Promotionsschrift, TU Munchen, 1968.
5. Hjorth, Olaf: "Ein Beitrag zur Frage der Festigkeiten und des Verbundverhaltens von Stahl und Beton bei hohen Beanspruchungsgeschwindigkeiten"; Dissertationsschrift, TU Braunschweig, 1975.
6. Der Bundesminister für Raumordung, Bauwesen und Stadtebau: Bau- und Wohnforschung, Forschungsbericht zum Thema "Verhalten von Beton bei sehr kurzer Belastungsgeschichte" (T 692).
7. Forschungskolloquium "Stoßartige Belastung von Stahlbetonbauteilen", Universität Dortmund,19. Sept. 1980.
8. Noakowski, R: "The Behaviour of the Compressed Zone of Concrete Industrial Chimneys", 4th International Symposium on Industrial Chimneys, The Hague, May 1981.

Commentary No. 3

Wind Load

Table of Contents

1 Wind Speed

The hourly mean wind speed has been chosen as the basis for the wind load. After estimation of the turbulence intensity the wind load is calculated by the "gust factor" method.

1.1 Basic Wind Speed

The basic wind speed used in deriving wind loads is the wind speed measured at 10 m above ground at the chimney location and averaged over one hour which has a probability of being exceeded of 0.02 in any one year. Values of the basic wind speed valid for a given location should be obtained from meteorological stations. When wind speeds have been measured over periods shorter than 50 years the correction factor given in Figure 1 may be used to extrapolate the basic wind speed.

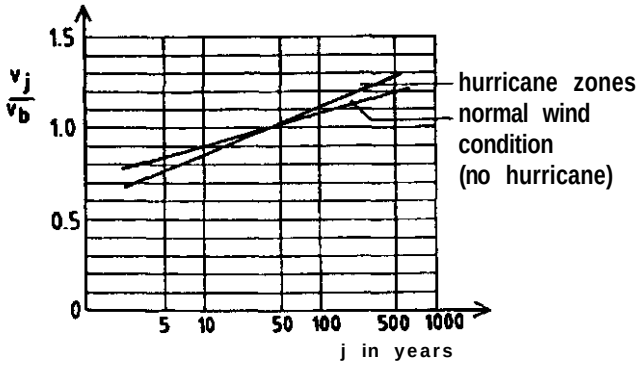

Figure 1 - Ratio between values of mean wind speed vj with a return period of j years and the Basic Win Speed v_b with a return period of 50 years

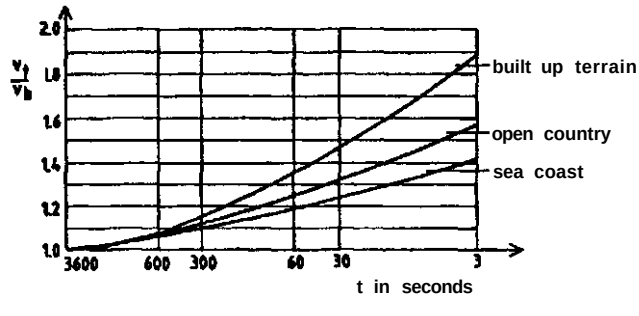

Figure 2 - Ratio between wind speeds v_t with averaging time t and the hourly Basic Wind Speed v_b as a function of averaging time

If the averaging time is less than one hour, the hourly mean may be determined using Figure 2. In this figure the ratio between the hourly mean and shorter averaging periods of the wind speed is given for various types of terrain.

1.2 Wind maps

In case results of wind speed measurements are not available, an indication of the basic wind speed is given in the Figures 3, 4, 5 and 6 for Europe, North America, Asia and Australia.

The values indicated for Europe must be divided by 1.05 to give the mean hourly wind speed v_b.

1.3 The Influence of the Topography

Section 7.2.2.2 of the Model Code requires the determination of a topographical factor k_t in case of non-flat country for the determination of the design wind speed. For certain topographical situations, a method for the determination of k_t is given in [4]. An approximation of the diagrams in [4] is described in the following. The method is valid for topographical situations which can be adequately described by three values U, ψ_U and ψ_D as in Figure 7.

The factor kt is obtained by formula (1)

$$\begin{aligned} k_t &= \left(1 + 1.2 * \psi_E * \left(1 - x/U_E - z/U_E\right)\right) && \text{if } \psi_D \geq 0.05 \\ k_t &= \left(1 + 1.2 * \psi_E * \left(1 - x/4U_E - z/U_E\right)\right) && \text{if } \psi_D < 0.05 \end{aligned} \qquad (1)$$

where

$$\psi_E = \begin{cases} \psi_U & \text{if } \psi_U \leq 0.3 \\ 0.3 & \text{if } \psi_U > 0.3 \end{cases}$$

$$U_E = \begin{cases} U & \text{if } \psi_U \leq 0.3 \\ 3.3 * h & \text{if } \psi_U > 0.3 \end{cases}$$

h height of hill or escarpment, see Figure 7

U horizontal length of upwind slope

x distance of chimney from crest

z height of considered position in chimney above ground.

If equation (1) gives a value $k_t < 1$, then $k_t = 1$.

1.4 Interfering Objects

The determination of the influence of interfering objects on the wind speed is complicated and may necessitate wind tunnel tests. In some cases the interference factor k_i may be estimated as follows:

a) if the height of the interfering object is less than half the chimney height, take $k_i = 1$

b) if the interfering object is an almost cylindrical structure,

$$\begin{aligned} k_i &= 1.25 - (0.15/9d) * a && \text{for } 6d < a \leq 15d \\ k_i &= 1.0 && \text{for } a > 15d \end{aligned} \qquad (2)$$

where

a distance of chimney down-wind from the interfering object (centre to centre)

d diameter of the interfering object

c) if a < 6d the factor k_i should be determined by wind tunnel testing or equivalent means.

2 The Gust Factor and the Peak Factor

The gust factor is taken from Davenport [5], and the peak factor g is taken from Davenport [6].

The turbulence intensity i and the energy density spectrum E are taken from ESDU [7] for a surface roughness parameter z_0 = 0.06 m.

3 The Static Equivalent of the Wind Load due to Gusts

Under the CICIND code the (static equivalent) wind load due to gusts varies linearly with the height. This causes an increase of the bending moment at high levels in the chimney compared with the normal gust-loading method. As a result the CICIND method gives a better approximation for the influence of the turbulence resulting from the higher modes of oscillation. This will give slightly higher moments at the chimney top whereas the values at chimney bottom are identical to those resulting from the standard procedure.

4 Vortex Shedding

In the first edition of this Commentary it was suggested that investigation of vortex shedding is not necessary if the following condition is fulfilled at all levels:

$$G/V \geq 2.0 KN/m^3 \qquad (3)$$

where

G weight of chimney above considered level

V corresponding volume of chimney.

The condition (3) corresponds to Scruton Number $Sc = \frac{2m\delta}{\rho d^2} \geq 15$

for damping logarithmic decrement of 0.05

To date vortex shedding of an amplitude which leads to unacceptable stress levels has not been observed in reinforced concrete chimneys which were correctly designed for wind loading in accordance with existing codes. The condition (3) is taken from observations mostly of steel chimneys and from wind tunnel tests. Condition (3) is thus not fully justifiable with the present knowledge of this phenomenon. To date no entirely satisfactory way of calculating across-wind response has been published. For the present the method of ACI 307-95 is recommended.

List of Literature

1. European Convention for Constructional Steelwork (E.C.C.S.): "Recommendations for the Calculation of Wind Effects on Buildings and Structures", September 1978.

2. Japan Association for Wind Engineering: Wind Resistant Design Regulations - A World List"; G.B. Fukyu - Kai, Tokyo, 1975.

3. Japan Association for Wind Engineering: Wind Resistant Design Regulations - A World List Supplement 1982"; G.B. Fukyu - Kai, Tokyo,1982.

4. Building Research Establishment Digest, No. 283: "Assessment on Wind Speed over Topography"; Building Research Establishment, Garston, Watford.

5. Davenport, A.G.: Note on the Distribution of the largest Value of a Random Function; Proc. I.C.E., Vol. 28, June 1964.

6. Davenport, A.G.: Gust Loading Factors; J. Struct. Div., Proc. ASCE, Vol. 93, ST3. June 1967.

7. Engineering Sciences Data Unit: ESDU Report 74031; London.

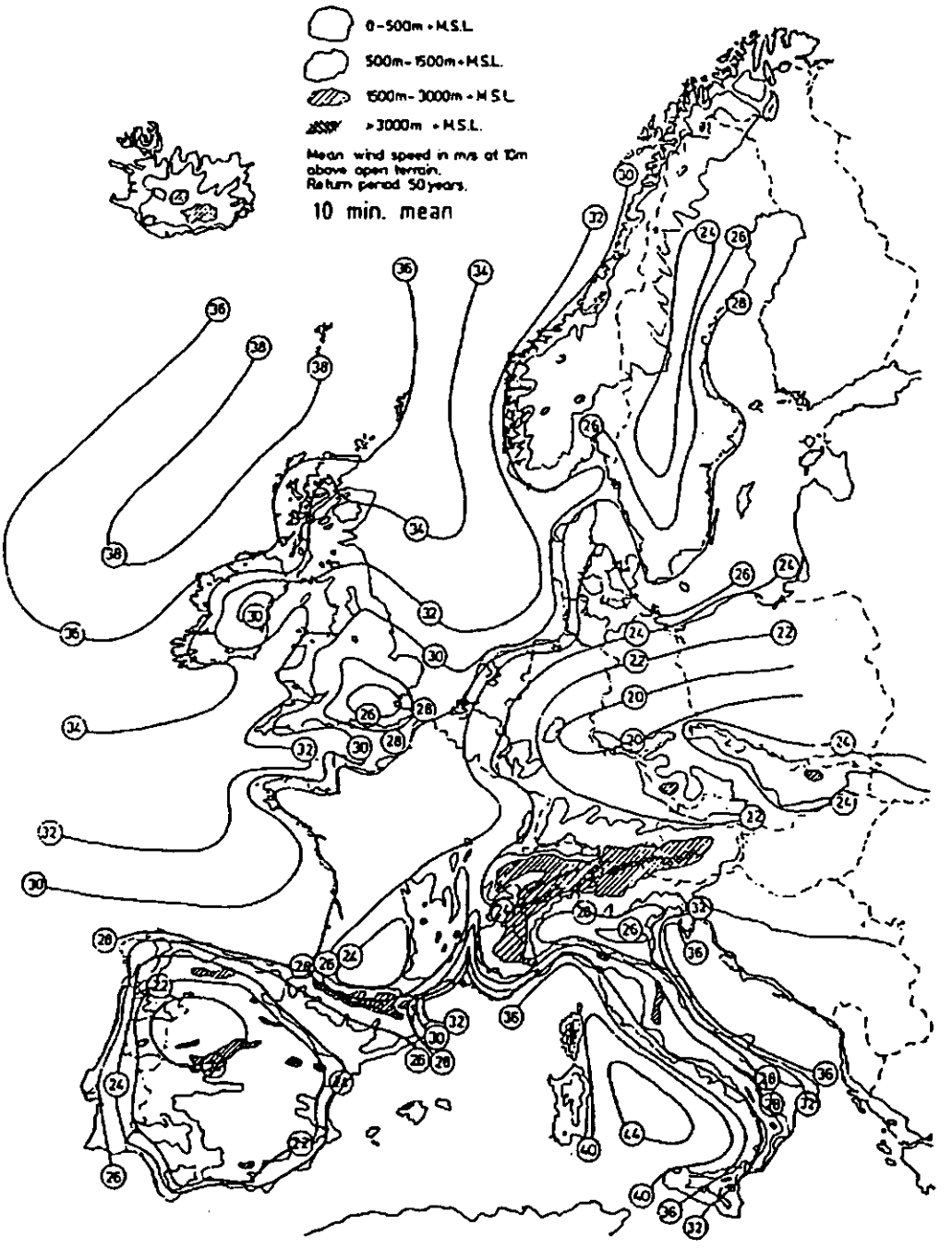

Figure 3 - Basic wind speeds v_b in m/s for Europe according to [1] (10m above ground, open country, 50 years return period)

NB - The values shown must be divided by 1.05 to obtain the mean hourly wind speed

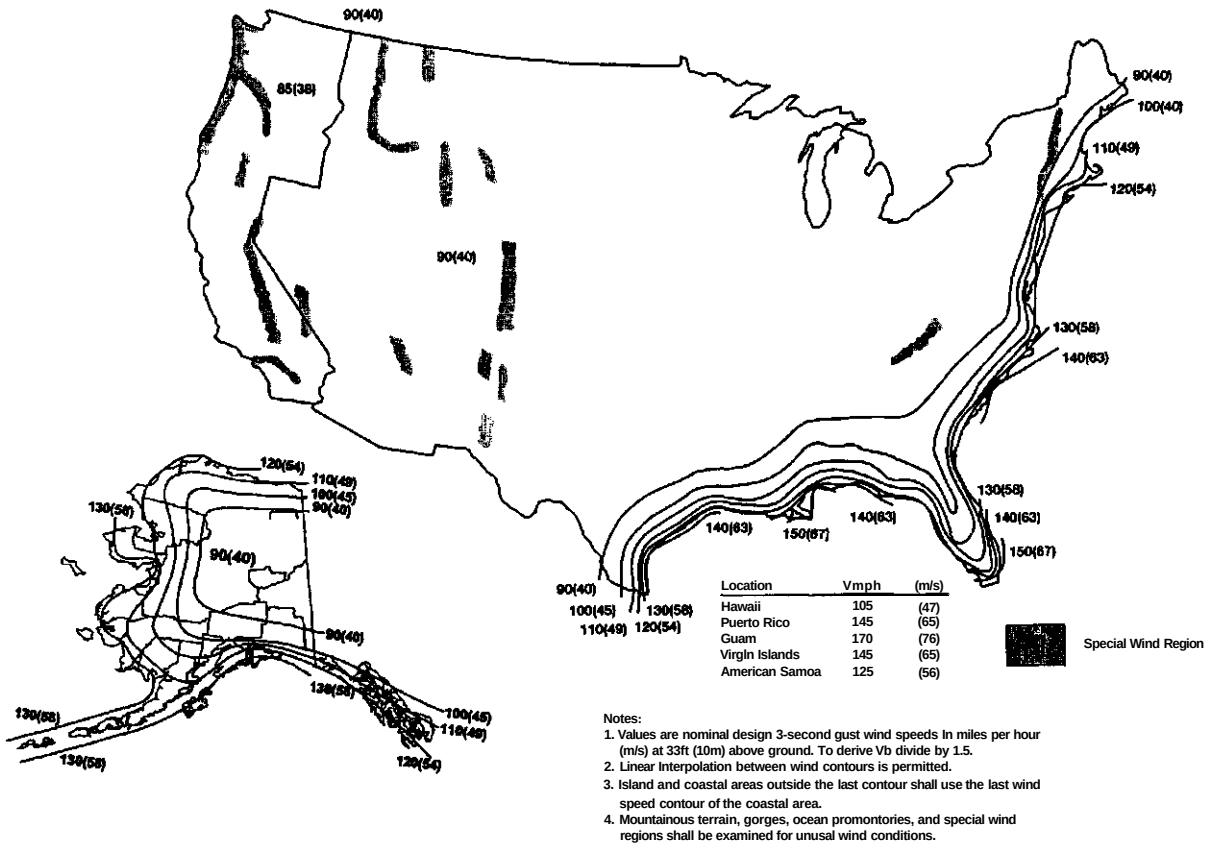

Figure 4 - Basic wind speeds v_b in m/s for USA according to [2] (10m above ground, open country, 50 years return period). Caution in the use of wind speed contours in the mountainous regions of Alaska is advised.

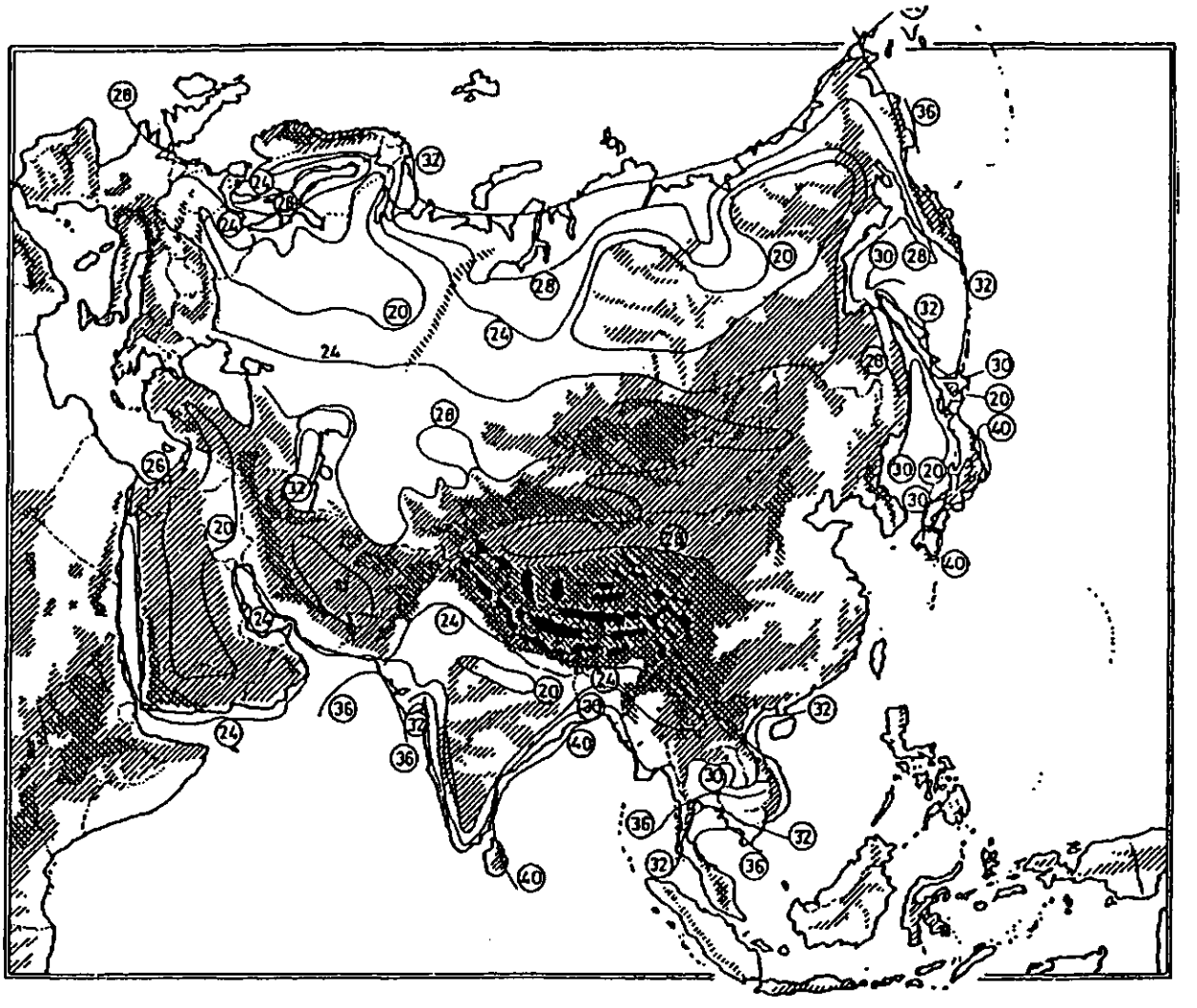

Figure 5 - Basic wind speeds v_b in m/s for Asia (10m above ground, open country, 50 years return period, hourly mean).

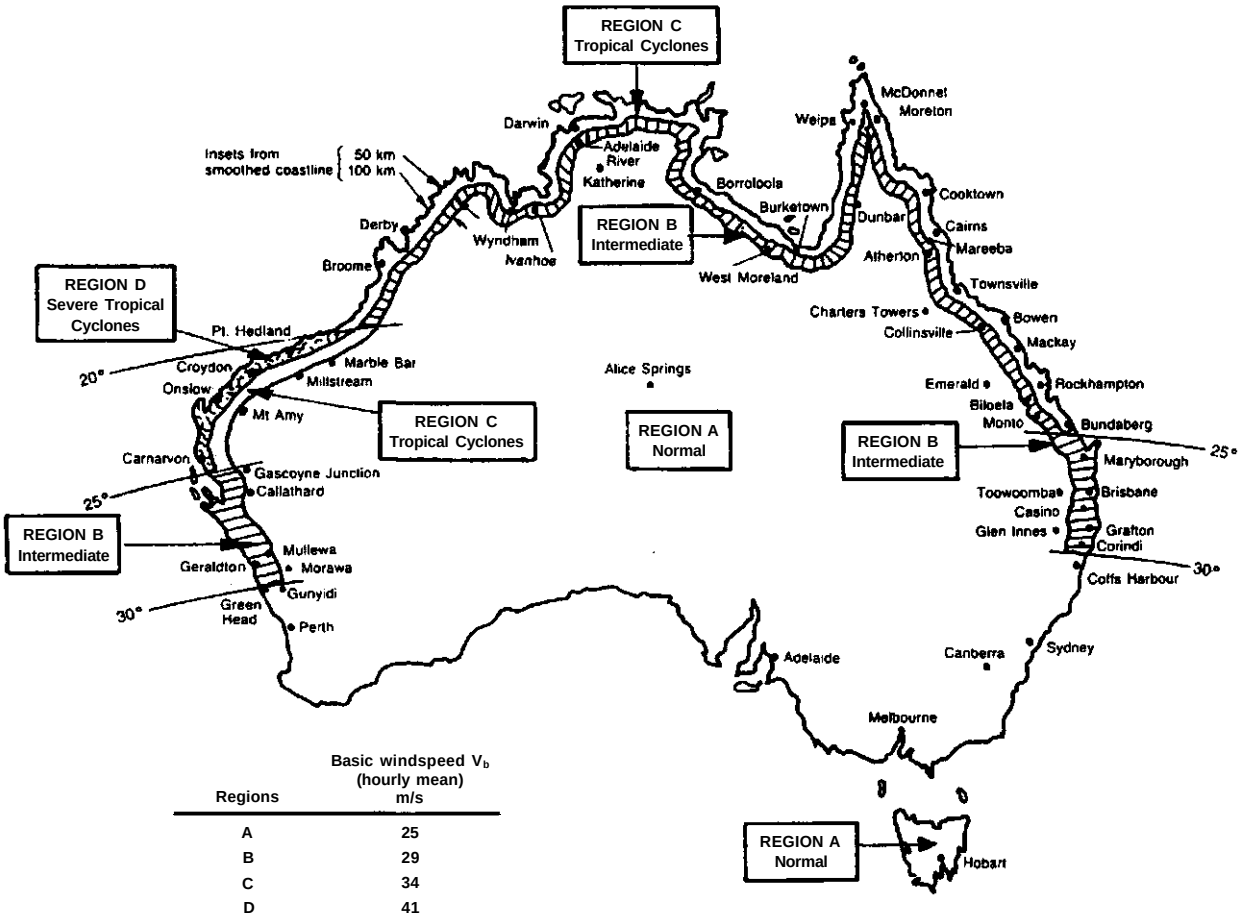

Figure 6 - Basic wind speeds v_b in m/s for Australia according to [3] (10m above ground, open country, 50 years return period, hourly mean).

Notes:

- Tropical cyclone-prone areas, shown hatched, are up to 50km inland from the coast north of Latitude 27°.
- Within the topical cyclone-prone areas all design velocities shall be multiplied by 1.15.
- Within the tropical cyclone-prone areas a minimum design velocity of 34m/s shall be used.

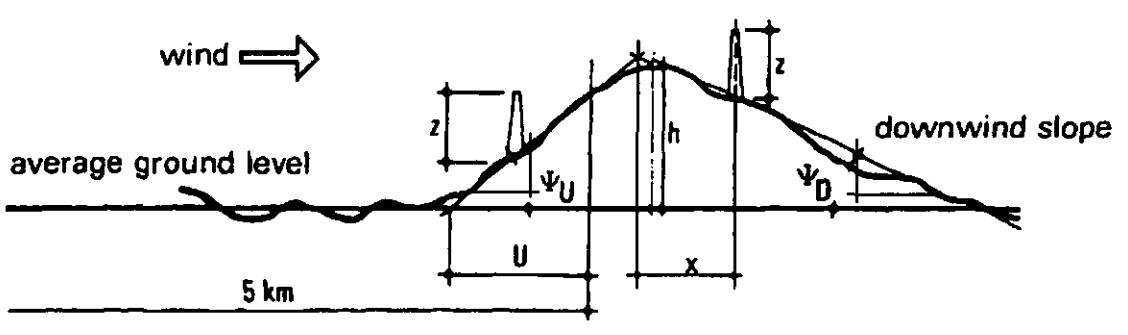

Figure 7 - Hill parameters for determining k_t

Commentary No. 4

Moments of 2nd Order

Table of Contents

1 Introduction

Chimney deflections are calculated by twice integrating the curvatures along the chimney height. Here - as opposed to proofs of load carrying capacity - the average material properties are the determining factors.

The actual stiffness of the tension zone of the shell is higher than that calculated assuming cracked sections everywhere. This "tension stiffening effect" results from the bond between concrete and reinforcement.

Both the importance of the material properties with respect to deformations and the decrease of the strains in the tension zone as a consequence of the tension stiffening effect are considered in the CEB-regulations [1] and in the German Chimney Code DIN 1056 [2].

In the following, the CICIND regulations and their application are described.

CICIND adopts the following safety factors:

- safety factors for materials for use in the calculation of deformations
  - • concrete $\gamma_{cu} = 1.20$
  - • steel $\gamma_{su} = 1.15$
- safety factors for loading
  - • permanent loads $\gamma_P = 1.00$
  - • wind $\gamma_W = 1.60$

2 Compression Zone

The deformation behaviour in the concrete compression zone is determined by the average modulus of elasticity of the concrete E_c.

The value for the modulus of elasticity of concrete is determined by the following CEB-equation [1] for the short-term behaviour.

$$E_c = 9500(f_{ck} + 8)^{0.33} \qquad (1)$$

(All values of f_c, f_s, E_c, E_s are in MPa in this Commentary.)

The tensile strength of the concrete is also taken from the CEB-regulations [1]:

$$f_{ct} = 0.3(f_{ck})^{0.66} \quad (2)$$

The resulting values of E_c and f_{ct} *are* given in Table 1. For the purpose of computing deformations these values should be divided by the safety factor $\gamma_{cu} = 1.2$

Table1: Material Properties of Concrete for the Calculation of Deformation

Concrete Quality	Modulus of Elasticity E_c MPa	Tensile Strength f_{ct} MPa
C25	30000	2.6
C30	31500	2.9
C35	33000	3.2
C40	34000	3.5
C45	35000	3.8
C50	36000	4.1

3 Tension Zone

The stress-strain relationship shown in Figure 1 is based on [3]. This tension stiffening law is greatly simplified compared with the law given in [3], but is always on the safe side with respect to the steel stresses.

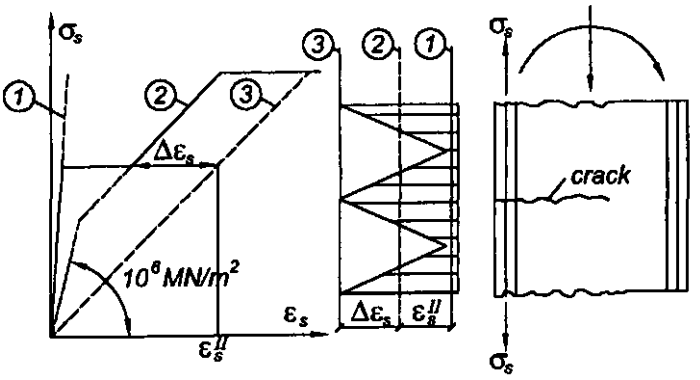

① state I without cracking
② mean conditions
③ state II

Figure 1 : Explanation of the Tension Stiffening Effect

In the following, a fictitious bar in the tension zone of a circular chimney cross-section is considered. The dotted line in Figure 1 is the "pure state II" condition which would arise if there were no tension stiffening effect. The solid line represents the mean stress-strain behaviour of the reinforcement lying in this bar. The tension stiffening effect causes a translation of the "pure state-II-line" towards the σ_s-axis by the amount $\Delta\varepsilon_s$. The magnitude $\Delta\varepsilon_s$ of the tension stiffening effect is determined from the following considerations:

- The steel stress just after cracking is:

$$\frac{f_{ct}}{\gamma_{cu}} * A_c = \sigma_s^{II} * A_s \rightarrow \sigma_s^{II} = \frac{f_{ct}}{\rho * \gamma_{cu}} \quad (3)$$

- The relation between $\Delta\varepsilon_s$ and the steel strain ε_s at the crack (see Figure 1) is:

$$\Delta\varepsilon = 0.5 * \varepsilon_s^{II} \quad (4)$$

where

$$\varepsilon_s^{II} = \frac{0.5 * f_{ct}}{E_s * \rho * \gamma_{cu}}$$

The simplified tension stiffening law is now constructed as follows:

- The first part is a straight line with slope 10^6 MPa up to the point where the tensile concrete strength is less than the concrete tensile stress and crack formation begins.
- From this point up to yield the value $\Delta\varepsilon_s$ describes the tension stiffening effect.
- After yielding the steel stress is constant.

Figure 2 shows the tension stiffening law prepared for practical use.

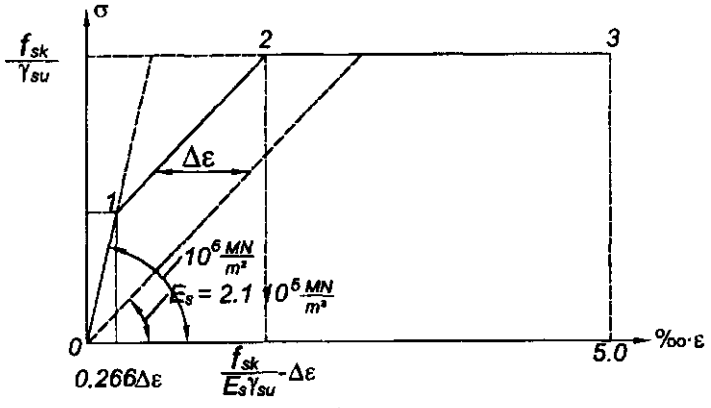

range0-1 $\sigma = 10^6\ \varepsilon$

range1-2 $\sigma = E_s\ (\varepsilon + \Delta\varepsilon)$

range2-3 $\sigma = \frac{f_{sk}}{\gamma_{su}}$

where

De *measure of the tension stiffening effect*

$$\Delta\varepsilon = \frac{0.4}{E_s}\ \frac{f_{ct}}{\rho_v\ \gamma_{cu}}$$

f_{sk} *yield stress of steel MN/mm²*
f_{ct} *tensile strength of concrete MN/mm²*
E_s *modulus of elasticity of steel MN/mm²*
ρ_s *ratio of vertical reinforcement*
γ_{cu} *partial safety factor for concrete*
γ_{su} *partial safety factor for steel*

Figure 2 : Tension Stiffening Law

4 Exact Determination of the Moments of 2nd Order

For the determination of the moments of 2nd order, the mean strains e_c and E, at the compressed and the tensioned edge of the cross-section are needed. Figure 3 shows a procedure to calculate these strains. The calculations are based on the concrete modulus EC fron equation (1), the tension stiffening law of Figure 2 and the following conditions of equilibrium

$$N = \sum_1^n \left(\sigma_c \frac{\pi d}{n} t + \sigma_s \frac{\pi d}{n} t\rho \right)$$

$$M = \sum_1^n \left(\sigma_c \frac{\pi d}{n} t + \sigma_s \frac{\pi d}{n} t\rho \right) \frac{d}{2} \cos \alpha \qquad (5)$$

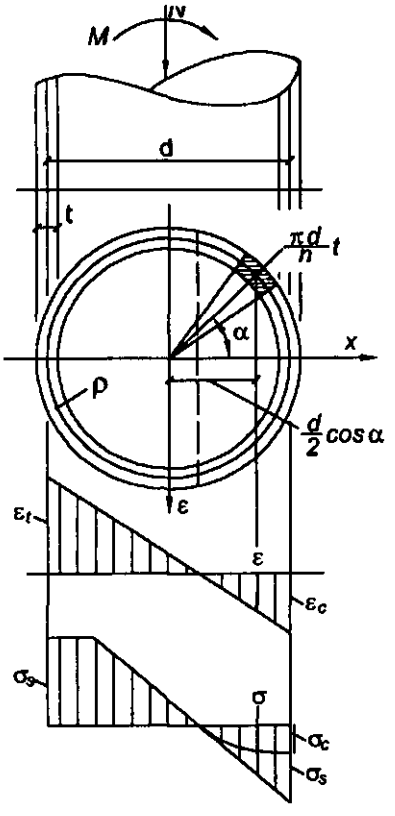

d *mean diameter*
t *wall thickness*
ρ *ratio of reinforcement*
concrete stress as a function ofe
σ_c *steel stress as a function of* e
strain at the individual section
ε

$$\varepsilon = (\varepsilon_t - \varepsilon_c) \frac{1-\cos\alpha}{2} + \varepsilon_c$$

ε_c *strain at the compressd edge*
ε_t *strain at the tensioned edge*
N *nonval force*
M *bending moment*
n *number of circumferential sections for numerical computation*
α *location angle for the individual section*

Figure 3 : Numerical procedure for the determination of the strains

Figure 4 illustrates the procedure by which the methodology of section 3 is applied to a complete structure.

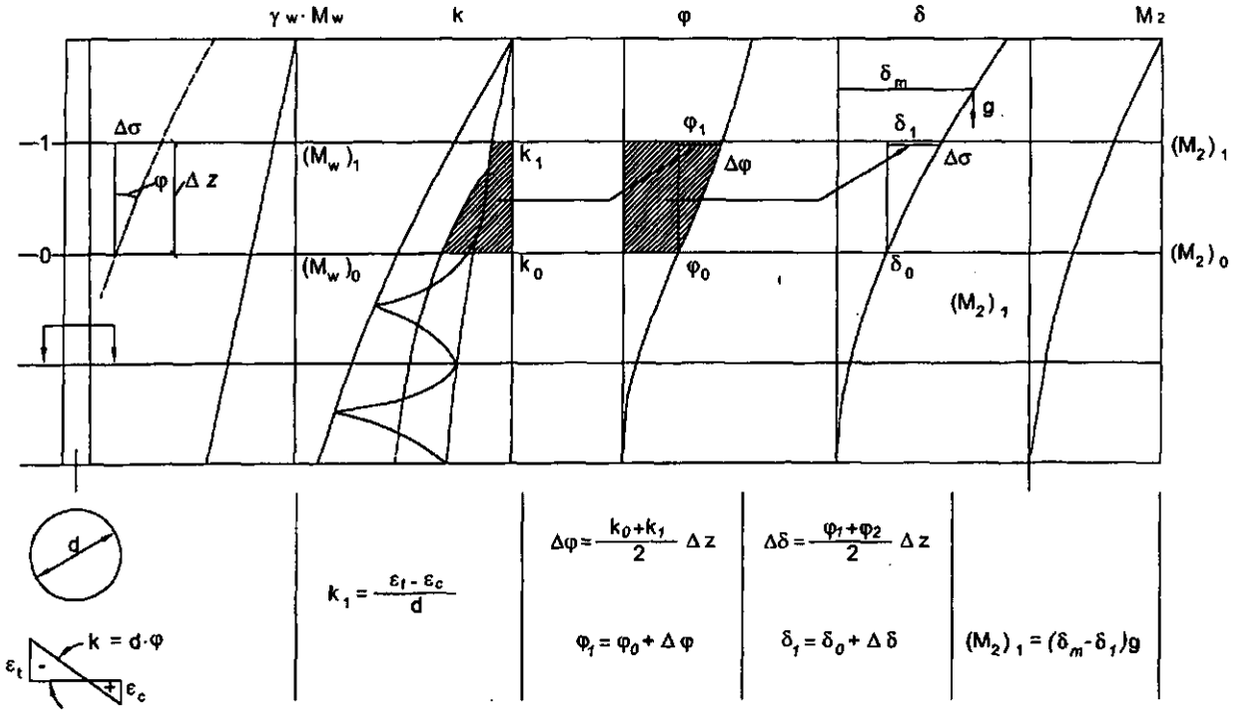

Figure 4 : Procedure for the exact determination of deflections and moment of 2nd order M_2 according to Ref. 3

The following section describes this procedure.

The rotation Φ is calculated by numerical integration of the curvature k. Further integration of the rotation Φ gives the deflection δ. The dead load g acting in the deflected position causes moments of 2nd order M_2.

In the next step of the iteration, the procedure is repeated with these moments added to the moments due to the ultimate limit state wind. If the design is viable the sequence converges, usually after 4 or 5 iterations.

The overall moment is the sum of the wind moment and the corresponding 2nd order moments. This value is to be used with the dimensioning diagrams in Commentary No. 6.

5 Approximation Method for the Determination of the Moments of 2nd Order

Moments of 2nd order can be determined approximately by the equation (8.9) in section 8.2.4.4 of the Model Code.

This approximation is developed following [4] & [5].

It is based on the assumption that the local load carrying capacity of the cross-sections is fully utilised and takes account of the tension stiffening effect.

The approximation method is valid for any combination of the following variables:

- concrete quality
- steel quality
- dimensions: height, diameter, shape and ratio of reinforcement of the shell
- loading: weight of the lining and wind.

6 Verification of the Approximation

The approximation has been checked for 60 chimneys for which the moments of 2nd order had been determined using the exact method described in section 4. The 60 chimneys were selected by combining the following parameters:

Concrete quality	f_{ck}	= 20, 25, 30,35, 40 MPa
Steel quality	f_{sk}	= 300, 400, 500 MPa

Dimensions:

height	h	= 100,200,300m
slenderness	h/db	= 15.0, 17.5, 20.0
ratio of conicity	d_b/d_t	= 1.66,2.0
waist fitting factor	w	= 2.0, 3.0

(w is an exponent which defines the shape of the external profile of the chimney)

ratio of reinforcement	ρ	= 0.0035 to 0.006

Loading:

wind velocity	V_b	= 16m/sto30m/s
thickness of liner	t_L	= 0.11 m
thickness of platforms	t_{PL}	= 0.5,1.0, 1.5m

A suitable combination of these parameters covers most existing chimney types.

Let k be the ratio of the exact moment of 2nd order to the approximate moment of 2nd order:

$$k = \frac{M_2 \text{ exact}}{M_2 \text{ approx}} \qquad (6)$$

The value k according to (6) has been computed for the 60 chimneys mentioned above, for 5 cross-sections in every chimney, altogether 300 values. Figure 5 shows the result and proves that the approximation is adequate since:

a) k is less than 1 in most cases

b) the majority of the cases are overestimated by less than 35 %.

The very few cases where k is larger than 1, i.e. where the approximation underestimates reality, can be tolerated for the following reasons:

a) CICIND uses a probabilistic safety concept. The increase of the failure probability for the few cases which underestimate reality is offset by the many cases which overestimate reality.

b) Moments of second order are normally in the range of 10 % to 20 % of the wind moment in ultimate limit state. An error in the moments of 2nd order of 35 % therefore represents an error of 5 % in the ultimate limit state moment.

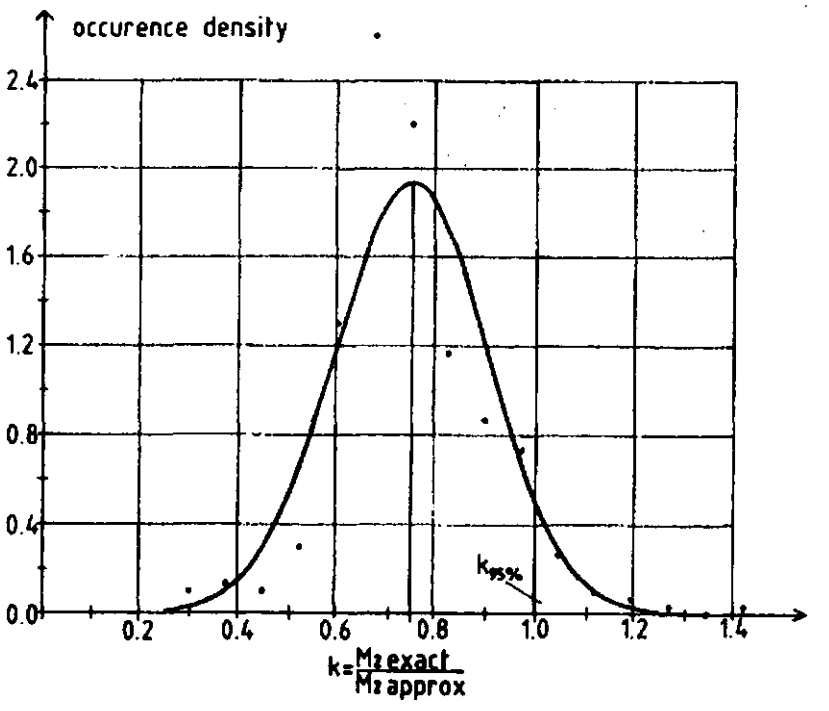

Figure 5 : Occurrence density of ratios of exact moment of 2nd order to approximate moment of 2nd order for 60m representative chimneys with 5 cross-sections per chimney

List of Literature

1. Comite Euro-International du Beton: "CEB/FIP International Recommendations for the Design and Construction of Concrete Structures. Principles and Recommendations."; 1978.

2. Deutsches Institut fur Normung: DIN 1056, "Solid Construction, Freestanding Stacks; Calculation and Design"; October 1984.

3. Noakowski, P., Kupfer, H.: "Stiffening Effect of Concrete in the Tension Area of Tower Structures"; 4th International Symposium on Industrial Chimneys, The Hague, May 1981.

4. Hees, G., Emrich, E, Zander, H.: "Untersuchungen zum Tragverhalten von Stahlbetonschornsteinen auf der Grundlage des Entwurfs zur DIN 1056"; Teil A, Forschungsvorhaben, Institut fur Bautechnik IV/1532/74, August 1982.

5. Noakowski, P.: "Simplified Determination of the Moments of Second Order" in Industrial Chimneys"; 4th International Symposium on Industrial Chimneys, The Hague, May 1981.

Commentary No. 5

Openings and Point Loads

Table of Contents

1 General

Stresses and strains are concentrated at corners of openings. This is illustrated by the results of calculations on plates as published by G. N. Savin [1] (see Figure 1).

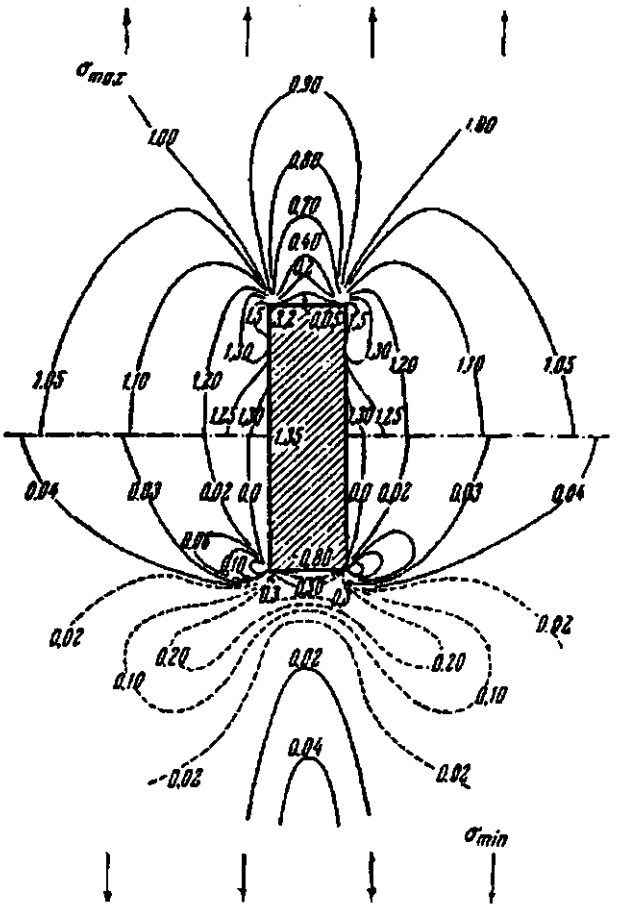

Figure 1 - Stresses and strains around openings according to Savin [1]

2 Virtual Openings

At a position 1.25b above the opening the stresses are not much below the stresses in the undisturbed area. This is the reason for the choice of size of a virtual opening shown in the following figure.

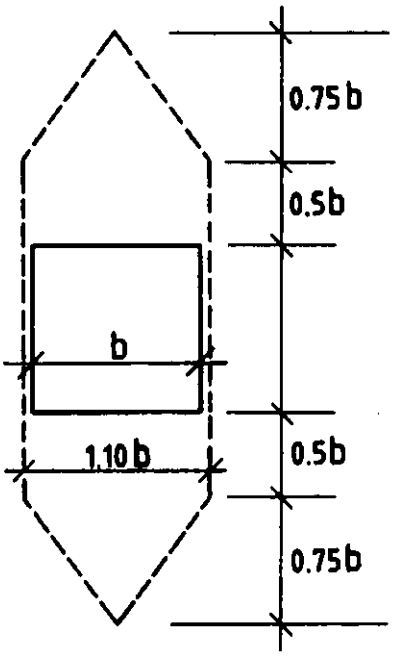

Figure 2 - Relation of real opening (solid line) to virtual opening (dashed line)

The requirement in respect of the distance between two openings:

$$a \geq 0.25(b_1 + b_2)$$

can be derived from Figure 1.

3 Horizontal Reinforcement

The total tensile force in the horizontal direction above and below an opening depends on the magnitude of the vertical stresses due to the normal force and the bending moment.

The tensile force is:

$$F_t = 0.1 b\, t(\sigma_c + \rho_v \sigma_s) \qquad (1)$$

where:

b	clear width of the opening
t	wall thickness
σ_c	vertical concrete stress in the undisturbed shell
σ_s	vertical steel stress in the undisturbed shell
ρ_v	ratio of vertical reinforcement

In the shell above and below an opening a bending moment m occurs acting to produce tension on the inside of the vertical sections at the middle of the openings:

$$m = 0.002 b^3 \frac{t}{d}(\sigma_c + \rho_v \sigma_s) \qquad (2)$$

where d mean diameter of the shell

4 Vertical Reinforcement

In the strength calculations, using an opening with a fictitiously large width of 1.1b leads to some extra safety. The total strain along the vertical line at the side of the opening must be equal to the total strain in the vertical direction along a parallel line some distance away. In the line along the side, there must be areas with reduced strains above and below the opening as high strains occur at the corners of the opening. In chimneys designed in accordance with the Model Code the compressive stresses due to the local strains in the corners are approximately 0.85 f_{ck} and the strains will be > 0.002. The large strains make the reinforcement very effective. The region where the strains exceed 0.002 (plastic state) can be seen in Figure 3. Extra vertical reinforcement amounting to 0.5 % of the area of this region must be added in a strip with length 0.5b and thickness t. This reinforcement must extend over a height equal to b plus a lap length at each corner.

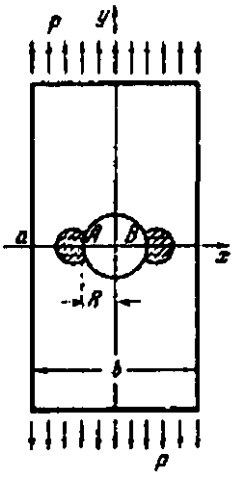

a) considered model

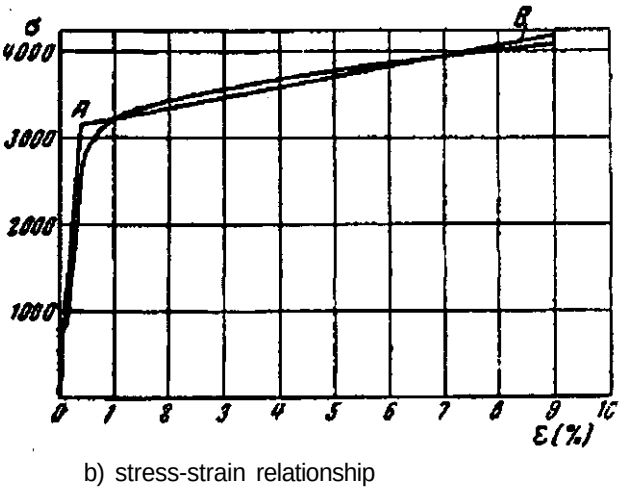

b) stress-strain relationship

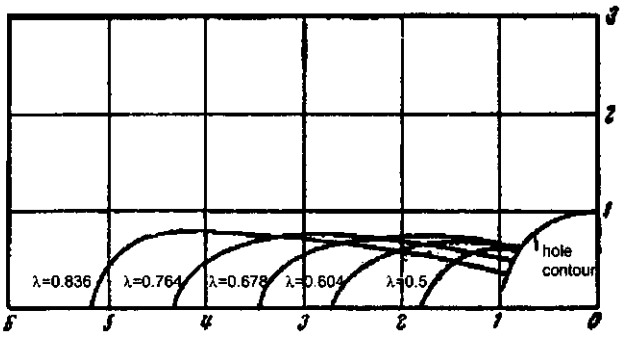

λ ratio of stress and yield stress in an undisturbed cross-section.

c) area with stresses above the yield stress
Point A in figures a) and b)

Figure 3 - Material plastification next to openings according to [1]

5 Local Moments from Point Loads on Corbels

The determination of moments produced from point loads in a shell is very complex. Analytical methods are not available. Measurements have been carried out (see [2]) which lead to the formulae (8.17 and 8.18) in the Model Code.

List of Literature

1. Savin, G. N.: Stress Concentrations around Holes", Pergamon Press, Oxford, London, New York, Paris, 1961.

2. Tooth.A. S., Kenedi, R. M.: The Influence Line Technique of Shell Analysis", International Colloquium of Simplified Calculation Method, Brussels, 1961.

Commentary No 6

Dimensioning Diagrams for Horizontal Cross Sections

Table of Contents

1 Description of the Dimensioning Diagrams

The 13 following dimensioning diagrams serve for the determination of

- the required wall thickness t and
- the required ratio of reinforcement p

in the horizontal cross-sections of the chimney shell.

For dimensioning the following initial data are needed:

- Material properties
  - characteristic steel strength f_{sk}
  - characteristic concrete strength f_{ck}
- Dimensions
  - shaft diameter d (at wall centre)
  - size of openings a (degrees) and number of openings (1 or 2)
- Loading for the ultimate limit state
  - permanent load N_u
  - total bending moment $M_u = \gamma_w * M_w + M_2$

  where:
  - M_w bending moment from wind
  - M_2 bending moment from deflection

The dimensioning diagrams are valid for f_{sk} = 400 MPa and for all f_{ck}

The diagrams are numbered according to the following key:

Diagram Figure No	Openings N x α	Validity
1	0	full cross sections
2	1x10°	cross sections with one opening
3	1 x 20°	
4	1 x 30°	
5	1 x 40°	
6	1 x 50°	
7	1 x 60°	
8	2x10°	cross sections with two equal opposed openings
9	2 x 20°	
10	2x30°	
11	2 x 40°	
12	2 x 50°	
13	2x60°	

Note: the angle α is that subtended by the actual opening, not the virtual opening of width 1.1b

The diagrams 1 to 13 are similar to the standard dimensioning diagrams for reinforced concrete cross-sections.

2 Use of the Dimensioning Diagrams

2.1 General

The cross-sectional forces in the dimensioning diagrams

n_u normalised normal force

m_u normalised bending moment

are limit state values.

2.2 Dimensioning with Respect to the Ratio of Reinforcement

The dimensioning with respect to the ratio of reinforcement is as follows:

a) The normalised cross-sectional forces n_u and m_u are computed from the values d, t, f_{ck}, N_u and M_u as shown in the diagrams.

b) The required value $\rho * f_{sk}/f_{ck}$ is read from the appropriate diagram, and from this the actual ratio of reinforcement p is computed.

2.3 Dimensioning with Respect to the Wall Thickness

For the determination of the required wall thickness the following procedure can be used:

a) The eccentricity η is found from N_u, M_u and d:

$$\eta = \frac{M_u}{N_u * d} \quad (1)$$

b) The straight line $m_u = n_u * \eta$ is drawn

c) The intersection of this straight line with the interaction curve for the chosen value of p gives the actual value for n_u

d) The wall thickness is given by

$$t = N_u / (\pi * d * f_{ck} * n_u) \quad (2)$$

3 Dimensioning Examples

Example 1 : Dimensioning with Respect to the Ratio of Reinforcement p

given: f_{sk} = 400 MPa
f_{ck} = 30 MPa
d = 20 m
t = 0.5 m
2 x (α = 40°)
N_u = 94.2 MN
M_u = $\gamma_w M_w + M_2$ = 1168.7 MNm

wanted: p

Dimensioning :

The normalised cross-sectional forces are:

n_u = 94.2 / (π * 20 * 0.5 * 30) = 0.100

m_u = 1168.7 / (π * 20^2 * 0.5 * 30) = 0.062

From diagram 11 read that

$\rho * f_{sk}/f_{ck} = 0.100$

Therefore

$\rho = 0.100 * 30/400 = 0.75$ %

Example 2: Dimensioning with Respect to the Wall Thickness t

given: f_{sk} = 400 MPa
f_{ck} = 30 MPa
d = 15 m
p = 0.75 %
α = 0
N = 44.80 MN
M_u = $\gamma_w M_w + M_2$ = 672.0 MNm

wanted: t

Dimensioning:

The normalised eccentricity is:

$$\eta = M_u / (N_u d) = 672.0 / (44.8*15) = 1.0$$

The normalised ratio of reinforcement amounts to

$$\rho * f_{sk} / f_{ck} = 0.0075*400 / 30 = 0.1$$

From diagram 1 at the intersection of η and p read that

$$n_u = 0.062$$

therefore

$$t = 44.80 / (\pi*15.0*0.062*30.0) = 0.51\ m$$

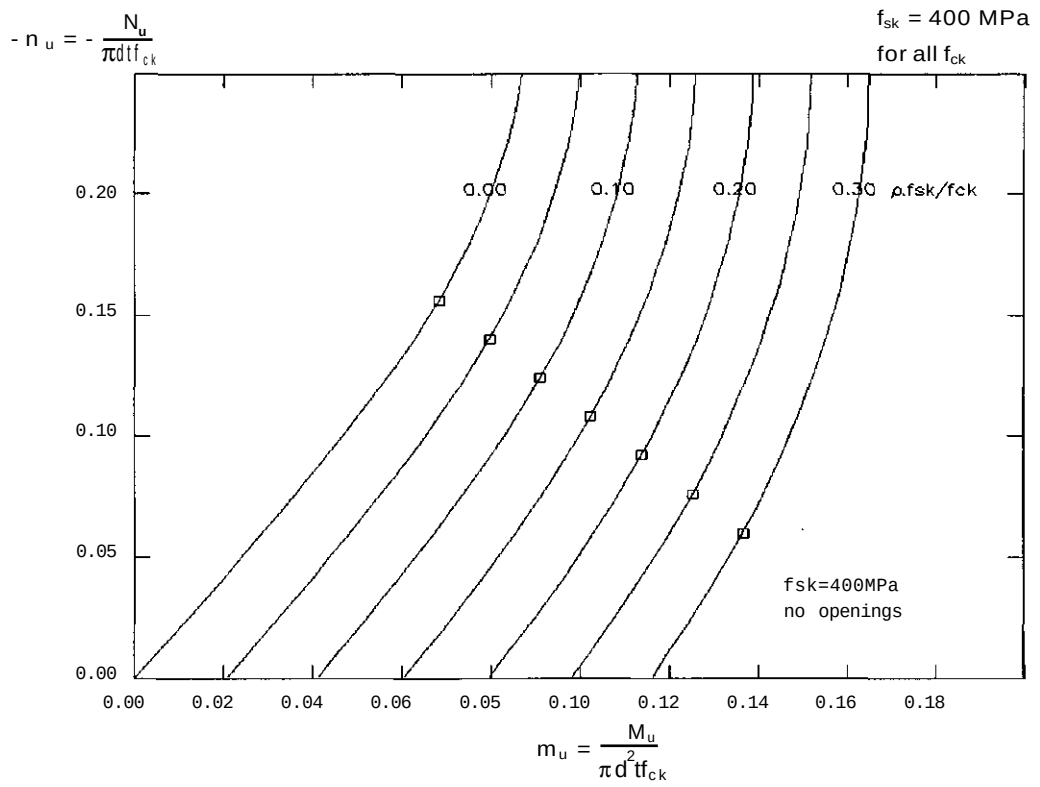

Fig. 1: Dimensioning Diagram for the Ratio of Reinforcement ρ and the wall thickness t of horizontal cross-sections with no openings

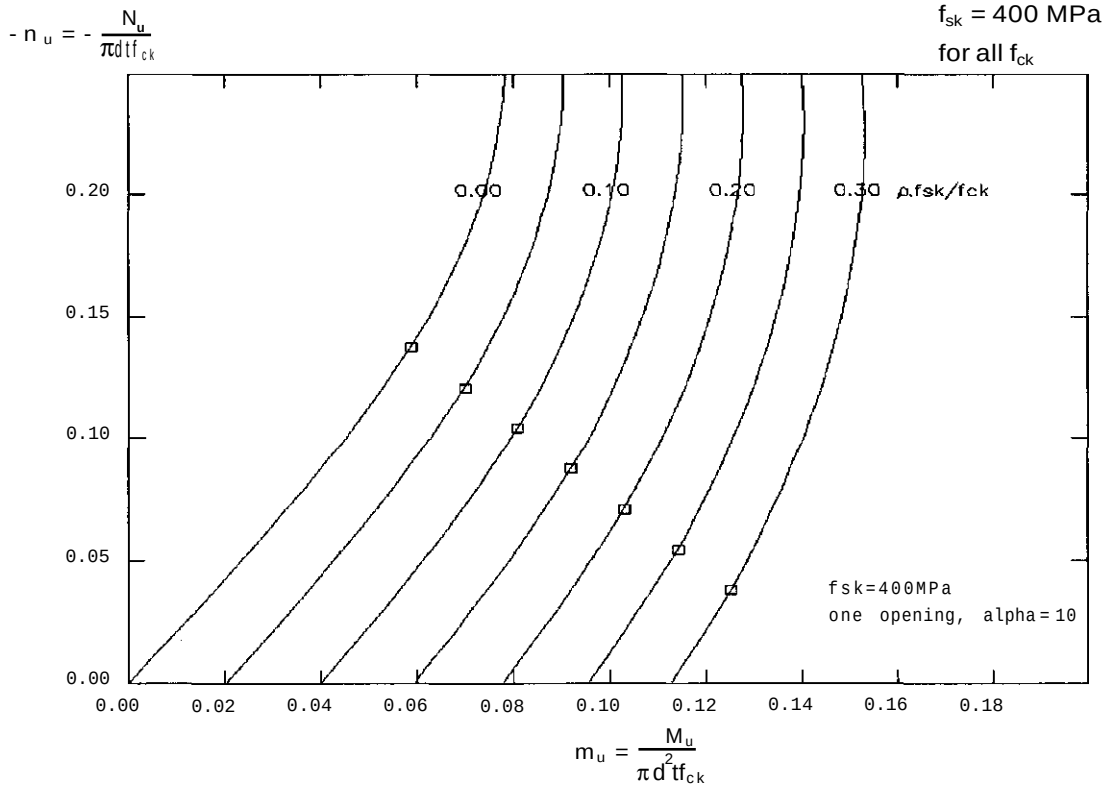

Fig. 2: Dimensioning Diagram for the Ratio of Reinforcement ρ and the wall thickness t of horizontal cross-sections with one opening of α= 10°

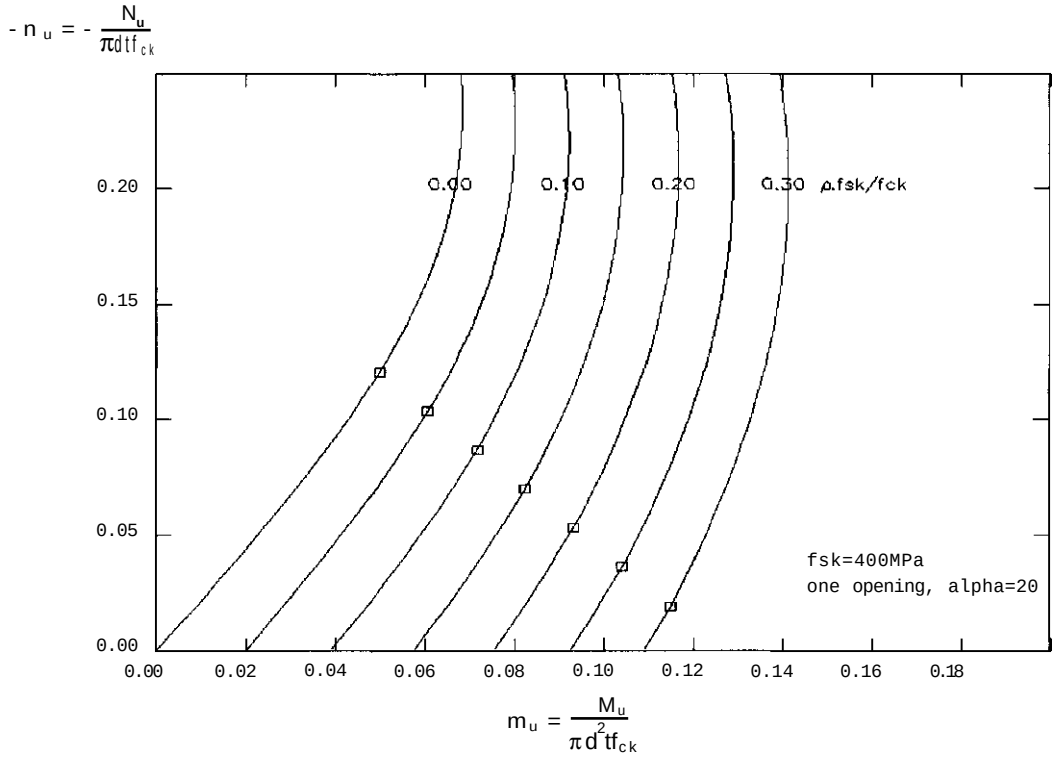

Fig. 3: Dimensioning Diagram for the Ratio of Reinforcement ρ and the wall thickness t of horizontal cross-sections with one opening of $\alpha = 20°$

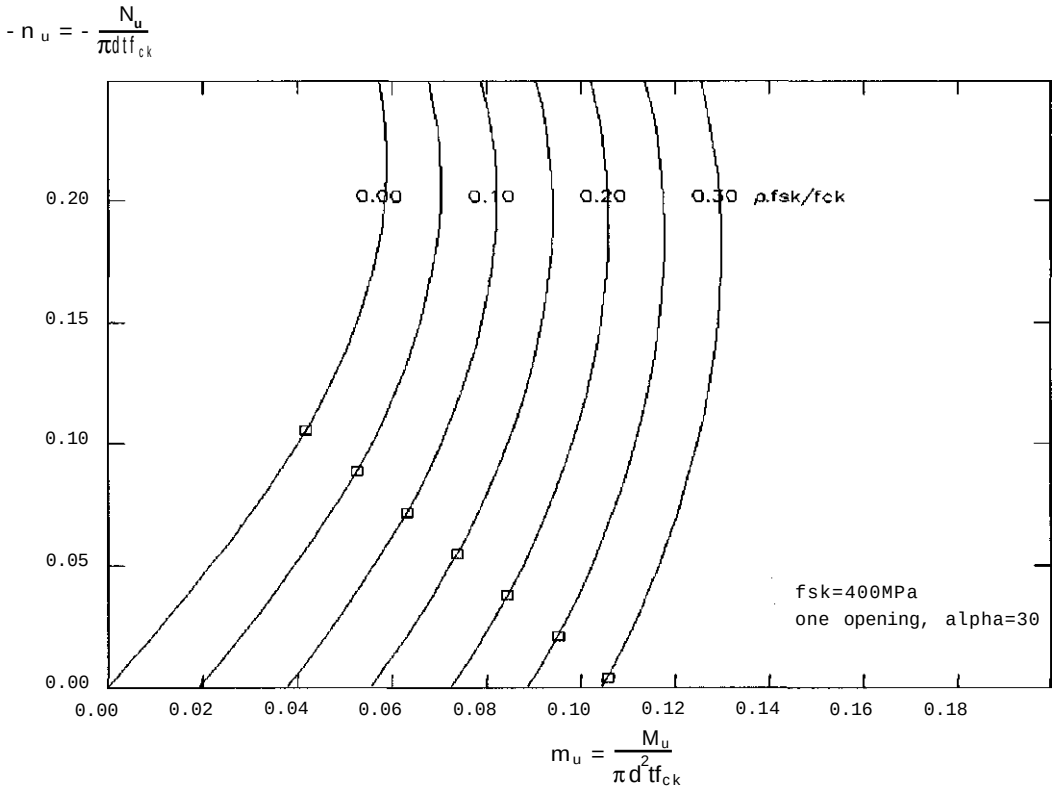

Fig. 4: Dimensioning Diagram for the Ratio of Reinforcement ρ and the wall thickness t of horizontal cross-sections with one opening of $\alpha = 30°$

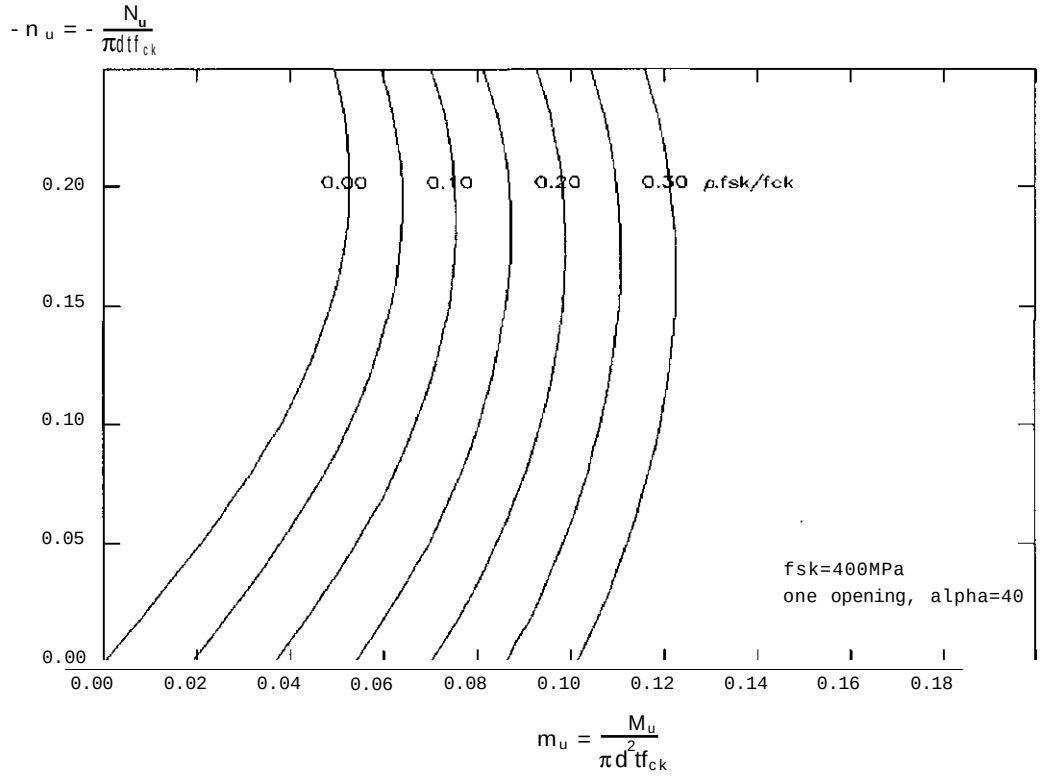

Fig. 5: Dimensioning Diagram for the Ratio of Reinforcement ρ and the wall thickness t of horizontal cross-sections with one opening of $\alpha = 40°$

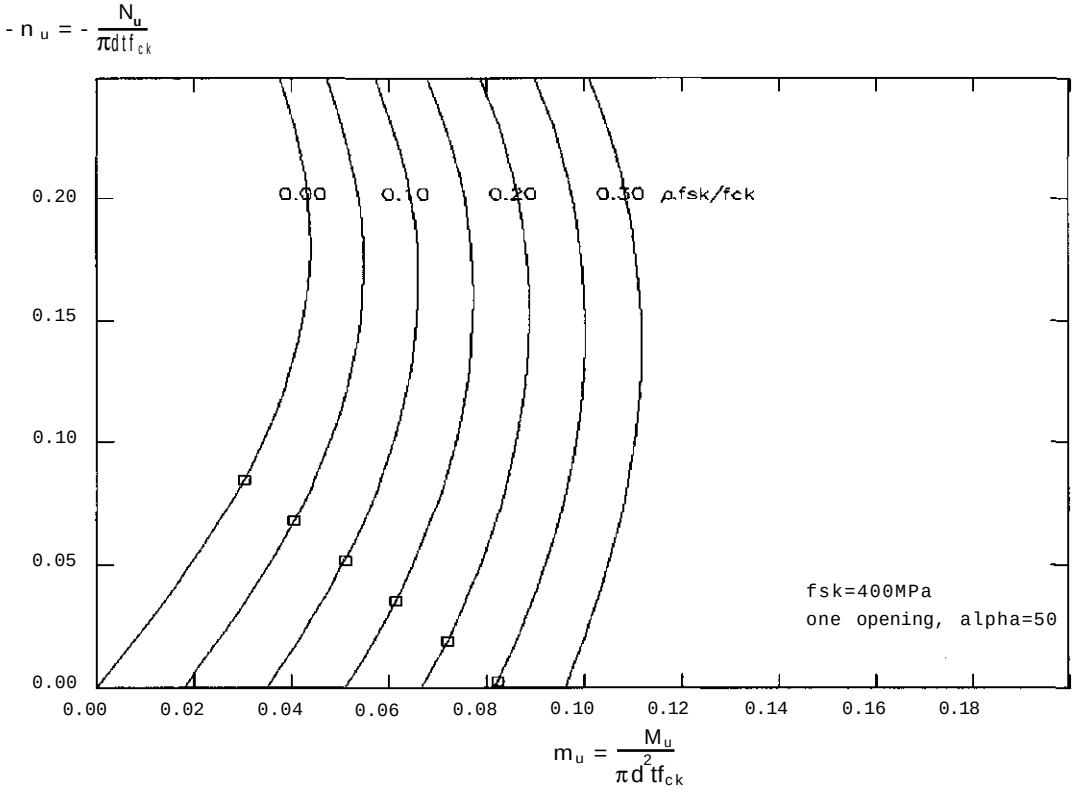

Fig. 6: Dimensioning Diagram for the Ratio of Reinforcement ρ and the wall thickness t of horizontal cross-sections with one opening of $\alpha = 50°$

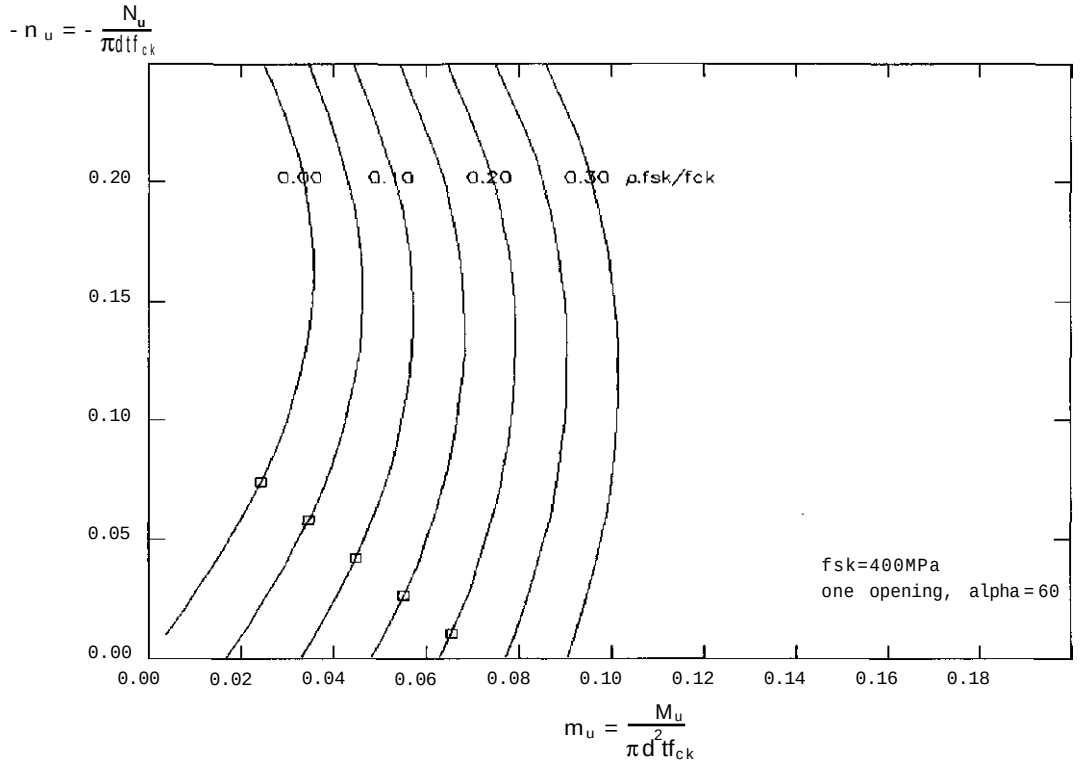

Fig. 7: Dimensioning Diagram for the Ratio of Reinforcement ρ and the wall thickness t of horizontal cross-sections with one opening of $\alpha = 60°$

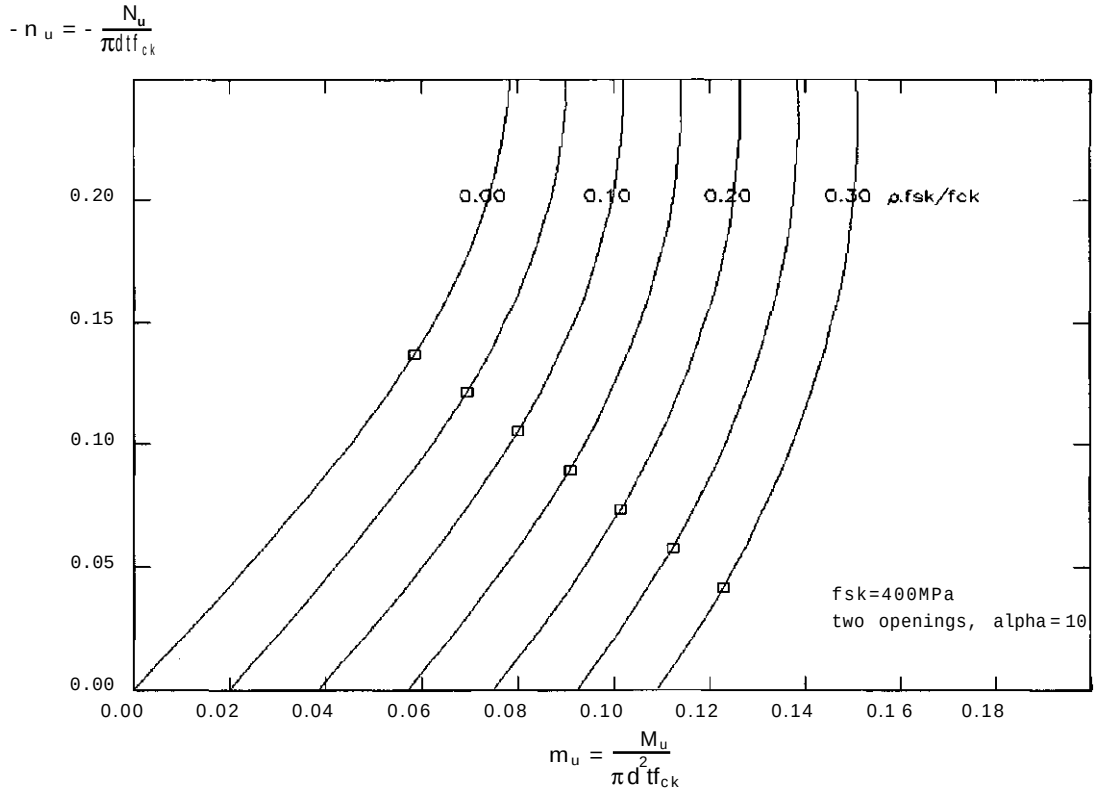

Fig. 8: Dimensioning Diagram for the Ratio of Reinforcement ρ and the wall thickness t of horizontal cross-sections with two opposed openings of $\alpha = 10°$

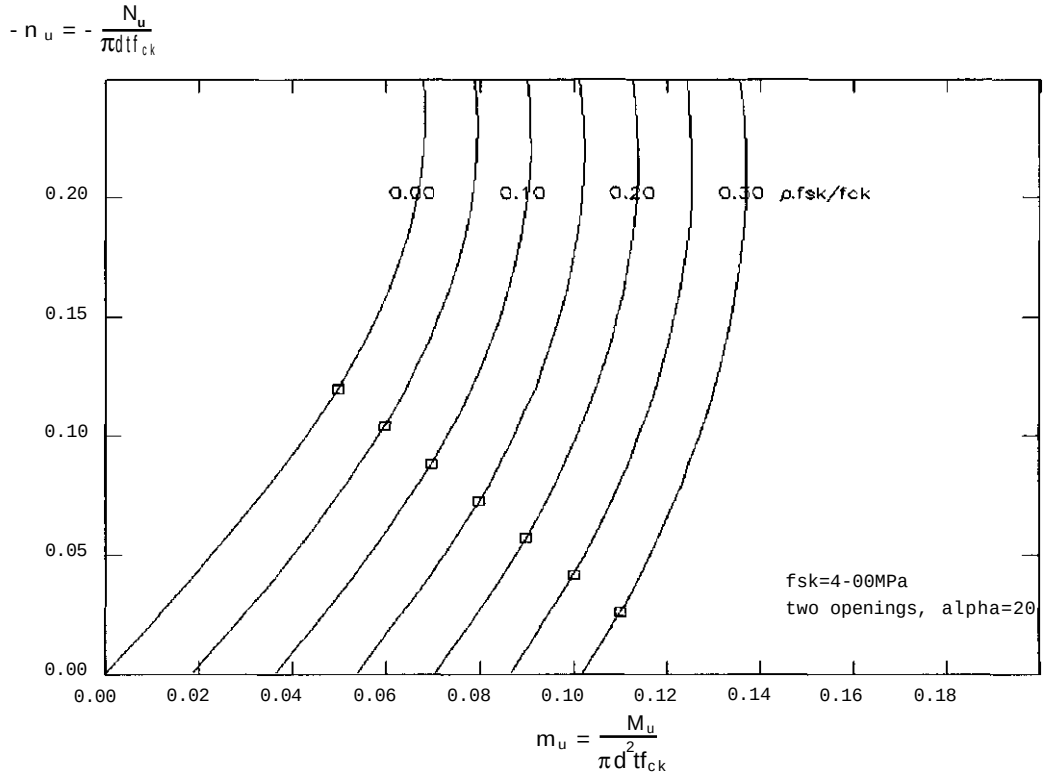

Fig. 9: Dimensioning Diagram for the Ratio of Reinforcement ρ and the wall thickness t of horizontal cross-sections with two opposed openings of $\alpha = 20°$

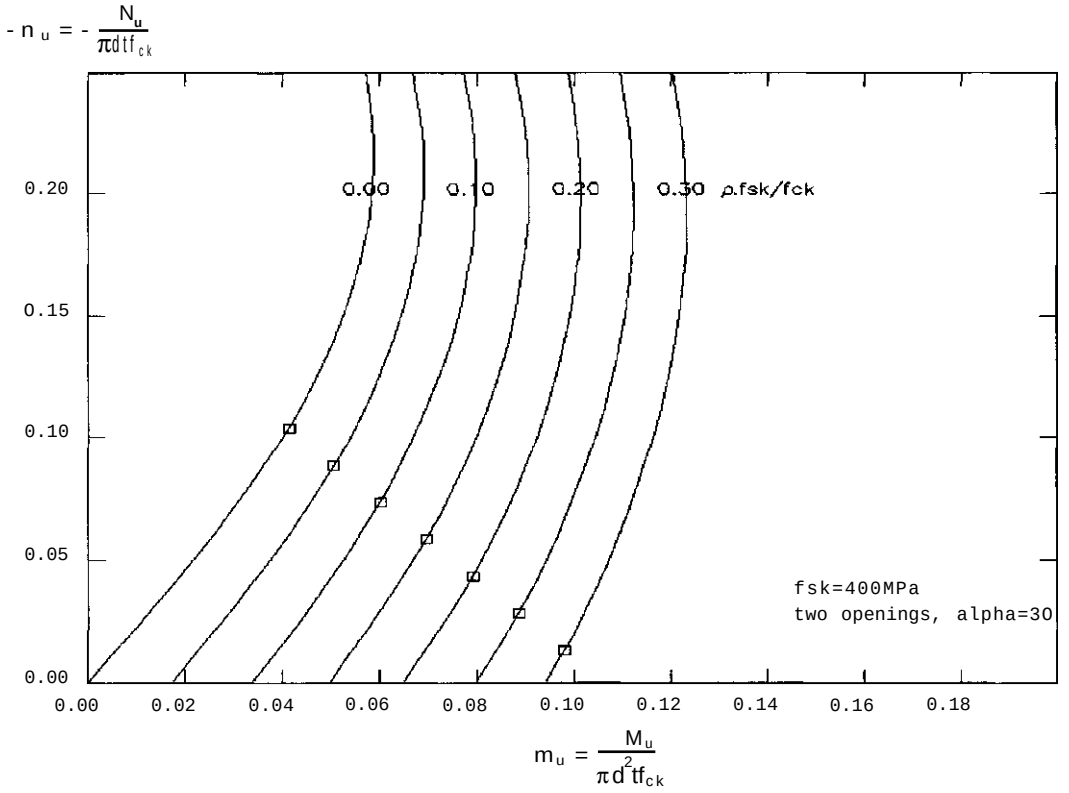

Fig. 10: Dimensioning Diagram for the Ratio of Reinforcement ρ and the wall thickness t of horizontal cross-sections with two opposed openings of $\alpha = 30°$

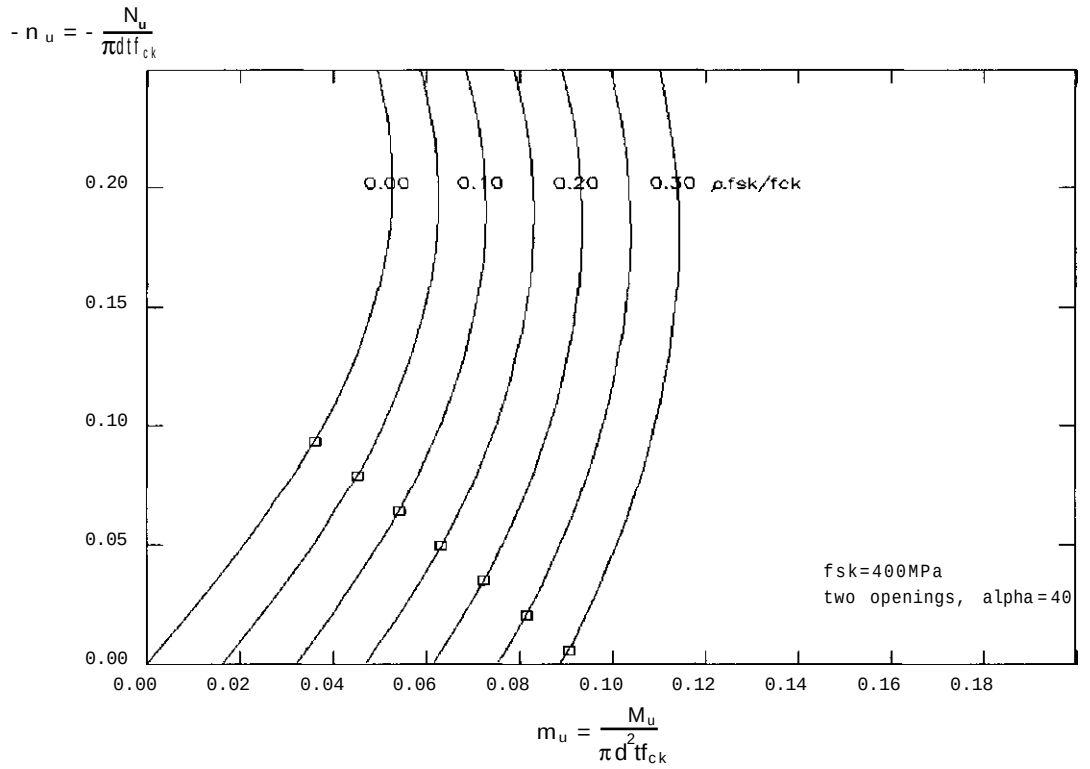

Fig. 11: Dimensioning Diagram for the Ratio of Reinforcement ρ and the wall thickness t of horizontal cross-sections with two opposed openings of $\alpha = 40°$

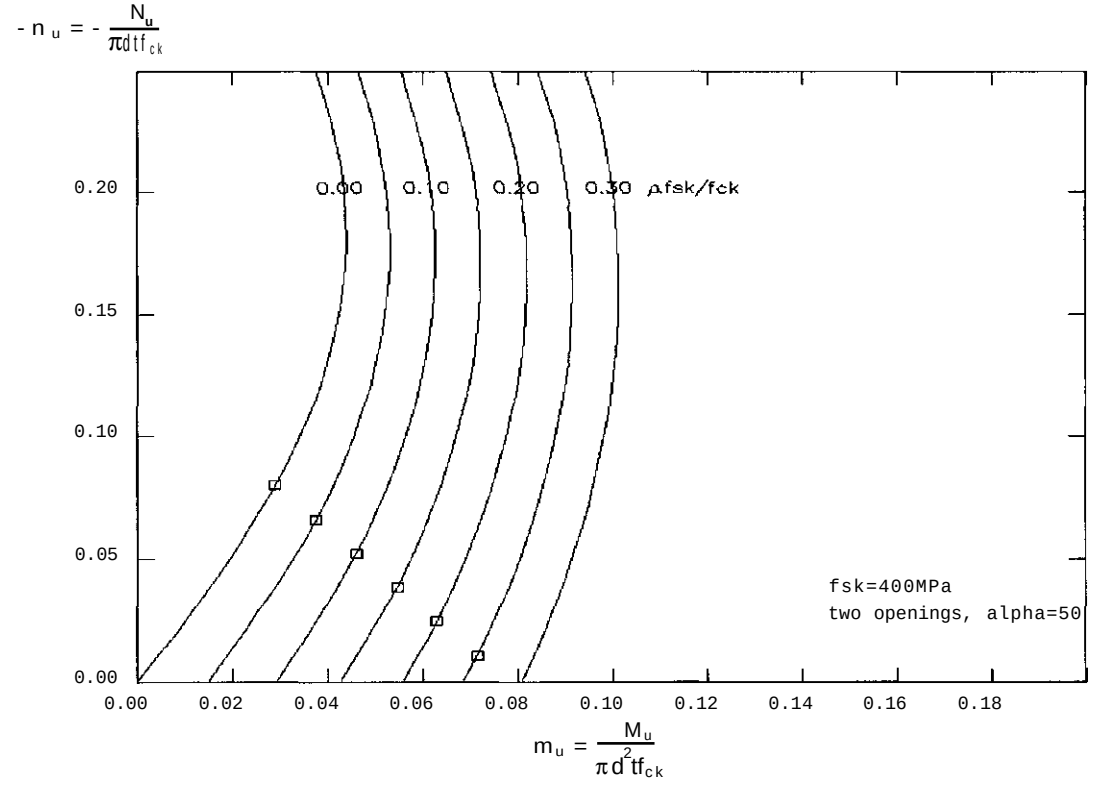

Fig. 12: Dimensioning Diagram for the Ratio of Reinforcement ρ and the wall thickness t of horizontal cross-sections with two opposed openings of $\alpha = 50°$

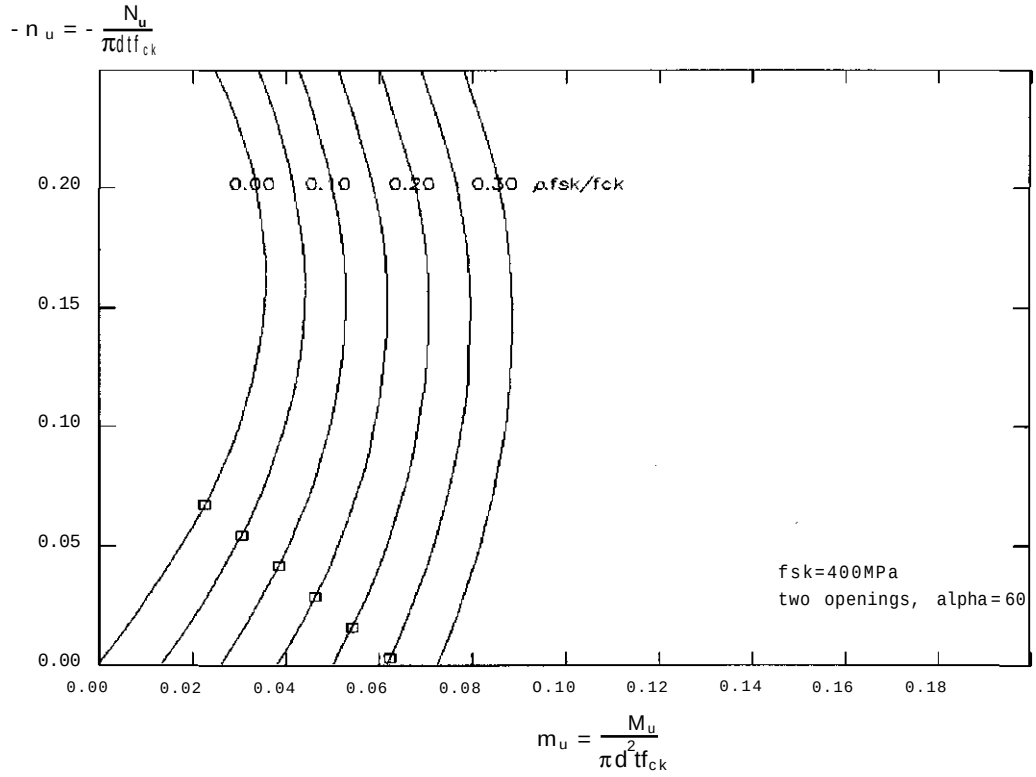

Fig. 13: Dimensioning Diagram for the Ratio of Reinforcement ρ and the wall thickness t of horizontal cross-sections with two opposed openings of $\alpha = 60°$

reinforcement is provided on each face of the shell even if the proportions are such that the stresses caused by the wind ovalling moment are negligible.

3 Cases for Design

Figure 1 shows those cases of thermal loading to be considered.

Case 1: horizontal bar

Case 2: vertical bar from the tension zone

Case 3: vertical bar from the neutral axis

Case 4: vertical bar from the compression zone

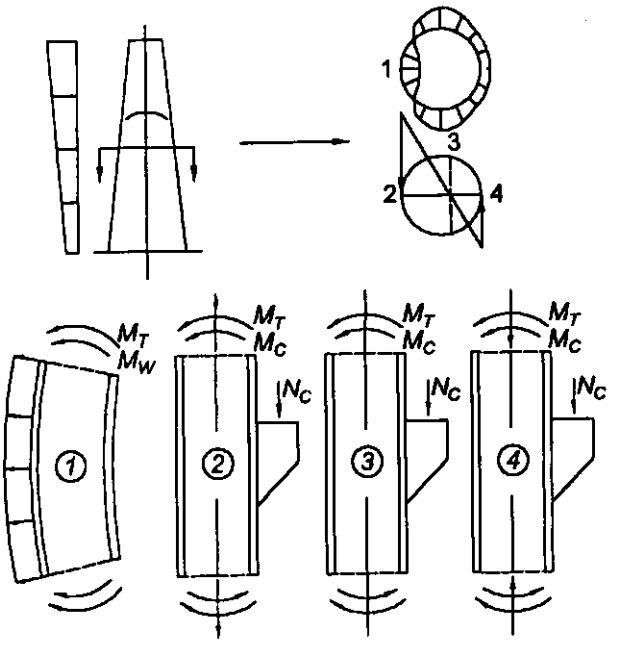

Case *1: horizontal bar*
Case 2: vertical bar from the tension zone
Case 3: vertical bar from the neutral axis
Case 4: vertical bar from the compression zone

Figure 1 : Bars taken out of the chimney shell to be designed for load and constraint due to temperature

Case 1: Generally, bending moments from temperature M_T and bending moments from wind M_w act on the horizontal bars from the shell. The circumferential reinforcement has to be designed for the simultaneous action of both bending moments.

Case 2: In the model of a vertical bar within the tension zone of the shell, the following actions may arise:

- M_T bending moment due to temperature difference
- M_c bending moment due to the load on a corbel
- N_σ tensile force due to permanent load and wind acting on the shell
- N_c axial force due to the load on a corbel.

The actions N_σ and N_c are combined into a single normal force N.

Case 3: At the neutral axis; same actions as case 2 except that N = 0.

Case 4: This represents a bar from the compressed zone; same actions as before, but N is negative.

The four cases described above can be generalised to one bar stressed by any normal force N from load and by two bending moments M_L and M_T. The bending moment M_L is due to load and the bending moment M_T is due to thermal effects.

4 Calculation of the Bending Moment due to Temperature

4.1 Fundamental Principles

The bending moments M_T due to temperature depend on the stiffness.

The calculation follows the principles shown in Figures 2 and 3. Figure 3 shows the following curvatures of the bar:

- k^I curvature in the region between cracks
- k^{II} curvature at the crack
- k^m mean curvature
- $\Delta k = k^{II} - k^m$ measure of the tension stiffening effect.

The values marked by the subscript 1 refer to the situation immediately after the formation of the cracks.

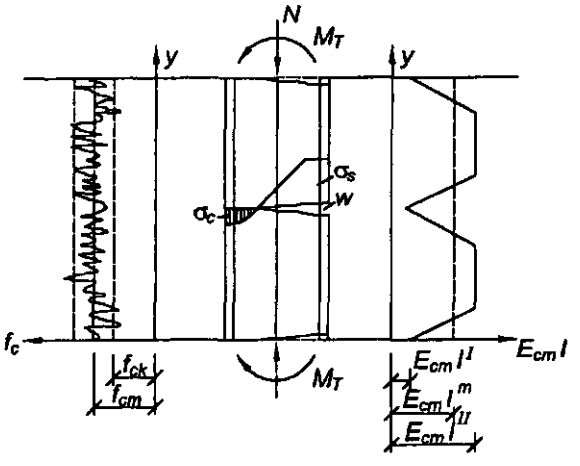

f_{ck} *characteristic strength of concrete*
f_{cm} *mean strength of concrete*
E_{cm} *mean modulus of elasticity of concrete*
I^I *2nd moment of area, state I*
I^m *mean 2nd moment of area*
I^{II} *2nd moment of area, state II*
w *crack width*

Figure 2 : Illustration of the necessary proofs for a model bar "cut out" of the chimney shell

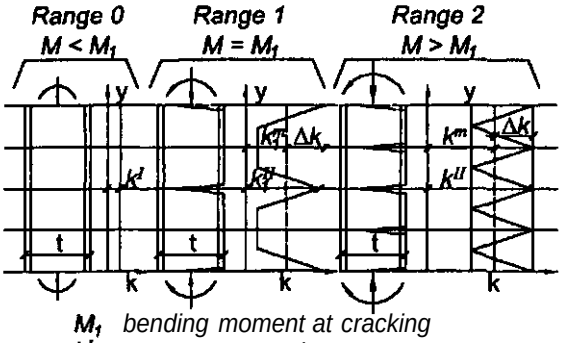

M_1 *bending moment at cracking*
k^I *curvature, state I*
k_1^m *mean curvature at cracking*
k_1^{II} *curvature at cracking, statell*
Δk *measure of tension stiffening effect*
k^m *mean curvature*
k^{II} *curvature, state II*

range 0 without cracks; statel

range 1 with single cracks; the distance of these cracks is so large that areas between the cracks are still in statel

range 3 with distinct cracks; the distance of these cracks is so small that no area between adjacent cracks Is still In statel

Figure 3 : Curvature of the considered bar belonging to three ranges of crack formation

Figure 4 shows the stiffness behaviour of the model bar

The following three ranges can be seen in Figure 4:

- Range O: $M_T + M_L < M_1$
  No cracks occur.
- Range 1: $M_T + M_L = M_1$
  In this range the cracks are isolated and the total bending moment from load M_L and temperature M_T is equal to the crack bending moment M_1. The reason for this behaviour is that with each increase of

ΔT for which the limiting value M_1 is reached a new single crack arises, which decreases the stiffness. The steel stress is reduced by the bond of concrete and steel between cracks. This induces tensile stresses in the concrete, eventually producing another crack.

- Range 2: $M_T + M_L > M_1$
  This range begins when the regions of disturbance from adjacent cracks touch each other.
  If now the moment is further increased, the steel stress will also increase, but the reduction of steel stress between cracks due to the transfer of forces from steel to concrete remains constant.
  Consequently the line for range 2 is parallel to the "pure state II" line.

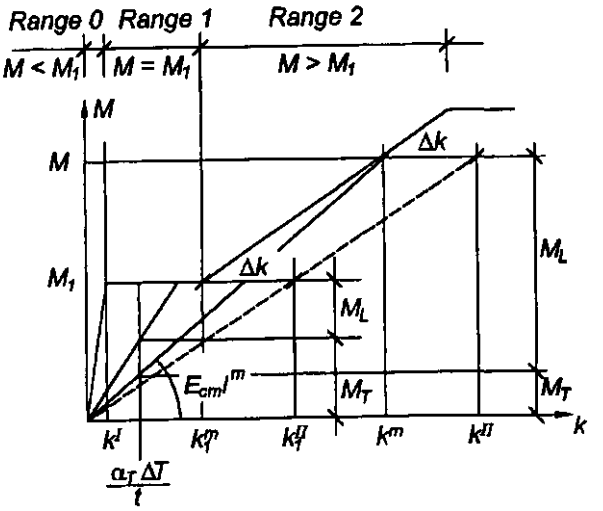

M_1 *bending moment at cracking*
M_T *moment from temperature*
M_L *moment from loading*
E_{cm} *mean modulus of elasticity of concrete*
I_m *mean 2nd moment of area*
k^I *curvature, statel*
k_1^m *mean curvature at cracking*
k_1^{II} *curvature at cracking, state II*
Δk *measure of tension stiffening effect*
k^m ***mean curvature***
k^{II} ***curvature, state II***

Figure 4 : Moment curvature relation of the considered bar divided into three ranges of crack formation

4.2 Calculation Method

4.2.1 Range O (uncracked model bar)

In this range the determination of the bending moment from temperature follows the simple relation

$$M_T = \frac{\alpha_T \Delta T E_{cm} I^I}{t} \qquad (1)$$

where

α_T	coefficient of thermal expansion
ΔT	temperature difference across the shell
E_{cm}	mean modulus of elasticity of concrete
I^I	2nd moment of area, state 1
t	wall thickness

4.2.2 Range 1 (model bar with single cracks)

In this range the bending moment from temperature is given by the following equation

$$M_T = M_1 - M_L \tag{2}$$

The crack moment M_1 is given by

$$M_1 = W^1\left(f_{ct} - \frac{N}{A^1}\right) \tag{3}$$

where

- N normal force
- M_L moment from load
- f_{ct} tensile strength of concrete (MPa)

$$f_{ct} = 0.45(0.85 - 0.20t)(f_{ck} + 8)^{0.66}\frac{2.6 + 24t}{1.0 + 40t} \tag{4}$$

- f_{ck} characteristic concrete strength (MPa)
- t wall thickness (m)
- A^I area of cross-section, state 1
- W^I section modulus, state 1

4.2.3 Range 2 (model bar strongly cracked)

The two following equations are used for the determination of the bending moment from temperature:

- equilibrium condition

$$\frac{\alpha_T \Delta T E_{cm} I^m}{t} = M - M_L \tag{5}$$

where I^m is the mean 2nd moment of area.

- compatibility condition

$$\frac{M}{E_{cm} I^m} = \frac{M}{E_{cm} I^{II}} - \frac{0.5 M_1}{E_{cm} I^{II}} \tag{6}$$

The total bending moment M and the mean 2nd moment of area I^m can be determined by these two equations.

The values of E_{cm} and I^{II} are calculated as follows:

a) E_{cm} is the mean secant modulus of the stress-strain relationship of concrete according to the parabolic behaviour of concrete.

$$E_{cm} = 850(1 + 250\varepsilon_N)(f_{ck} + 8) \tag{7}$$

where ε_N is the strain from the normal force.

b) The 2nd moment of area I^{II} and the section modulus W^{II} are calculated from the following equations:

$$I^{II} = \frac{1}{3}x^3 + Atx^2 - 2Bt^2x + Ct^3 \quad (8)$$

$$W^{II} = I^{II}/(t - x - t_1) \quad (9)$$

where

$x = At\left(\sqrt{1 + 2\frac{B}{A^2}} - 1\right)$ (height of compression zone)

$A = n(\rho_1 + \rho_2)$

$B = n(k_1\rho_1 + k_2\rho_2)$

$C = n(k_1^2\rho_1 + k_2^2\rho_2)$

$k_1 = (t - t_1) / t$

$k_2 = t_1 / t$

$n = E_s / E_{cm}$

$r_1 =$ ratio of reinforcement in the tension zone

$r_2 =$ ratio of reinforcement in the compression zone

$t_1 =$ concrete cover to the reinforcement axis

The method for the determination of I^{II} described above is strictly valid only for a state of pure bending. Nevertheless, it can be used for eccentricities $\eta = \left|\frac{M}{N\,t}\right| > 1$

5 Ultimate Limit State

The two types of loading causing bending moments M_L and M_T give rise to fundamentally different behaviour in the ultimate limit state. As this is approached the moment M_L remains constant, whereas the moment M_T decreases. The effect can be seen most clearly by considering case 2 in regions where the moment M_L is zero. Initially the strain difference caused by the thermal gradient gives rise to unequal stresses in the inside and outside reinforcement, but when the reinforcement yields under increasing wind load the stresses in the two layers are both equal to the yield stress. In the ultimate limit state the reinforcement strains become so large that there is no concrete compressive stress and M_T falls to zero. A similar argument can be applied to case 4, where consideration of the material law for concrete (Model Code fig. 6.1) shows that M_T falls to zero as the ultimate limit state is approached provided that the strain difference between the two faces is less than $(-\varepsilon_{cu} - 0.002)$. Given the coefficient of thermal expansion $\alpha_T = 10^{-5}$ and $-\varepsilon_{cu} = 0.003$ this condition is not reached until $\Delta T = 100K$.

These considerations lead to the conclusion that for the ultimate limit state the temperature difference can be allowed for by reducing the strain at which the concrete is deemed to fail by $0.5\,\alpha_T\Delta T$.

6 Serviceability Limit State

Yield of the reinforcement caused by tension in the serviceability limit state must be prevented as it will result in wide cracks which do not close when the load is reduced.

For vertical sections this requires that

$$M < M_y$$

where

M moment due to the characteristic wind and temperature difference

M_y moment at which the tensile reinforcement yields.

In the case of horizontal sections this condition may be ignored because of the high ultimate wind load factor and the creep caused by the permanent load.

7 Calculation of Crack Width

The width of vertical cracks is determined by following the principles shown in Figure 5.

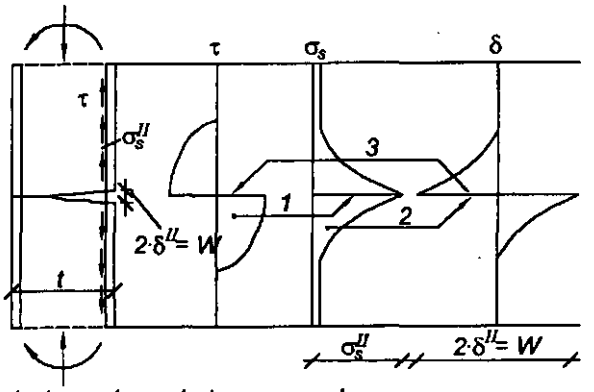

Figure 5 : Relations for the determination of the crack width

The chain of relations shown in Figure 5 is as follows:

a) The sum of the bond stresses τ gives the steel stress σ_s at the crack.

b) The steel stress σ_s divided by the modulus of elasticity of the steel E_s gives the displacement between the steel and the concrete at the crack.

c) The displacement δ is related to the bond stress T by the bond law (10)

$$\tau = 0.5(f_{ck} + 8)^{0.67} \delta^{0.12} \qquad (10)$$

The principles developed above were used to develop formula (11) relating the bar diameter Φ to the characteristic crack width w_k.

$$\Phi = 0.40 * 10^6 \frac{(f_{ck} + 8)^{0.67}}{\sigma_s^2} w_k^{1.12} \qquad (11)$$

where

Φ bar diameter (mm)

w_k characteristic crack width, $w_k = 1.3\ W_m$ (mm)

w_m mean crack width

σ_s post-cracking steel stress resulting from bending moment causing cracking.

Now, if f_{ct} is the tensile strength of concrete and p is the ratio of reinforcement on each face, $\sigma_s \approx 0.2 f_{ct}/\rho$. Substituting this in (11) and solving gives equation (12)

$$\rho_{min} = 0.2 f_{ct} \sqrt{\frac{\Phi}{0.40 \cdot 10^6 (f_{ck} + 8)^{0.66} w_k^{1.12}}} \quad (12)$$

where f_{ct} is given by equation (4).

Then the maximum bar spacing on each face is given by

$$s = \frac{\frac{1}{4}\pi\Phi^2}{1000 t \rho_{min}} \quad (13)$$

where

s bar spacing (mm)

t concrete thickness (m)

Equations (11) to (13) are identical with equations (9.1) to (9.3) of the Model Code.

8 Practical Design

The analysis can be considerably simplified in many cases, particularly as the characteristic wind and thermal loads are unlikely to occur simultaneously.

8.1 Horizontal Sections

For practical design it is considered that the small reduction in strength of the section can be ignored for $\Delta T < 60K$. This permits the use of the dimensioning diagrams of Commentary 6.

The dimensioning diagrams at the end of this section may be used to calculate the vertical reinforcement required in the neighbourhood of a corbel where the moment M_L Is non-zero.

8.2 Vertical Sections

The ultimate limit state requires that

$$M_{uh} > \gamma_{wh} M_{wh} \quad (14)$$

where

M_{uh} ultimate resistance moment

M_{wh} characteristic ovalling moment (Model Code section 8.3.1)

γ_{wh} ultimate wind load factor for ovalling

This is equation 8.14a in the Model Code

As shown in section 6 the serviceability limit state requires that

$$M_y > M$$

where

M_y moment for which $\sigma_s > f_{sk}$

In practice it is found that for values of $\Delta T <$ 60K, this can be approximated by

$$M_{uh} > M_1 \quad (15)$$

This is equation 8.14b in the Model Code.

Commentary No. 7

Superposition of Effects from Thermal and Other Actions

Table of Contents

1 Introduction

The chimney shell is subjected to thermal effects arising from two sources of heat:

- flue gases inside the chimney
- solar radiation (insolation).

The heat transfer across the wall leads to a temperature gradient. Because of the shell geometry the changes of curvature of the shell due to temperature difference are completely constrained in both directions. As a result both horizontal and vertical bending moments arise. In general these act together with bending moments and normal forces due to other loading. The magnitude of the thermal moment depends on the actual stiffness of the section. This stiffness depends on the properties of the cross-section and of the type and magnitude of the loading.

2 Computation Model

For the analysis we use as models horizontal and vertical bars which are imagined to be cut out of the chimney shell. The analysis considers the behaviour under short-term loading such as that due to insolation or furnace start-up. If the temperature gradient is sustained shrinkage and creep will combine to reduce the thermal stresses almost to zero within a few days. When the heat source is shut down the thermal stresses may be completely reversed. For this reason it is recommended that equal horizontal

9 Example

In the following, the section shown in Figure 6 is analysed by the simplified method, then checked by the detailed method.

Data

f_{sk}	400MPa
f_{ck}	30MPa
thickness t	0.4m
cover t_1	0.045 m
ΔT	50 K
M_{wh}	0.0610 MN
γ_{wh}	1.4

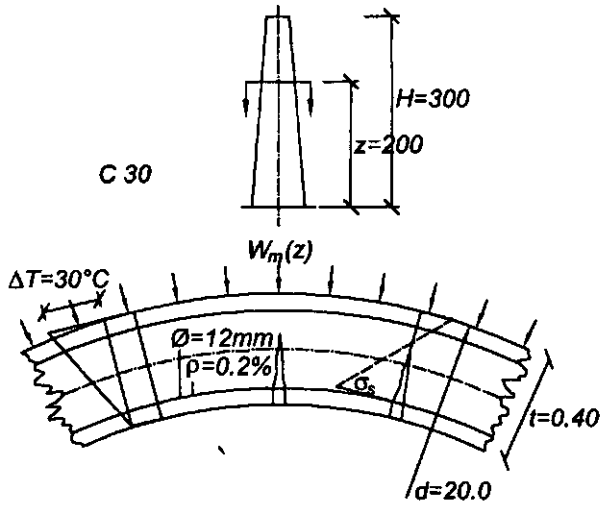

Figure 6 : Cross-section of a chimney with circumferential reinforcement: Example for explanation

(1) Ultimate limit state

Equation (14) $M_u > \gamma_{wh} M_{wh} \rightarrow M_u > 0.0854 \rightarrow \rho > 0.0018$

(2) Serviceability limit state

I^I	0.00559 m^4	(2^{nd} moment of uncracked section)
f_{ct}	2.811	from equation (4)

Equation (3) $M_1 = 0.0786 < M_u$

Therefore p = 0.0018 is sufficient.

(3) Crack width

w_k	0.2mm	
Φ	12 mm	(trial value for bar diameter)

Equation (12) $$\rho_{min} = 0.2 \cdot 2.811 \sqrt{\frac{12}{400000 \cdot 38^{0.66} \cdot 0.2^{1.12}}} = 0.0023 > \rho$$

therefore the reinforcement must be increased. Note that in this example the use of steel with greater yield strength would not lead to a reduction in the required reinforcement.

The spacing of 12mm bars is given by equation 13: $s = \frac{\pi \cdot 12^2}{4000 \cdot 0.4 \cdot 0.0023} = 123\ mm$

The detailed calculation for serviceability (section 4) gives:

E_{cm}	850(30+8) = 32300 MPa	from equation (7)
ρ_1	0.0018	
ρ_2	0.0018	
I^{II}	0.00048 m^4	from equation (8)

- equilibrium condition and compatibility condition

$40.4 \cdot I^m = M - 0.0610$ from equation (5)

$0.000031 \frac{M}{I^m} = 0.065 \cdot M - 0.0021$ from equation (6)

-results

M = 0.0912 MN

M_T = 0.0912-0.0610 = 0.030 MN

I^m = 0.00075 m^4

M_y = 0.0948 MN

Since $M_y > M$ the serviceability condition is satisfied. The crack width calculation is unchanged, so the required reinforcement ratio = 0.0023 as found by the simplified method.

List of Literature

1. Noakowski, P.: "Method of Design for Circumferential Reinforcement of Industrial Chimneys", 2nd Chimney Design Symposium and Exhibition, Edinburgh,30 March-1 April 1976.
2. Noakowski, P.: "Die Bewehrung von Stahlbetonbauteilen bei Zwangsbeanspruchung infolge Temperatur", Deutscher Ausschuss fur Stahlbeton, Verlag W. Ernst & Sohn, Berlin, 1978.
3. Kupfer, H., Noakowski, P.: "Untersuchung der vertikalen I Temperaturrisse in Schäften von Industrieschornsteinen aus Stahlbeton", Kongressband der 3. Internationalen Schornstein-Tagung, Vulkan-Verlag Essen, 25./26. Okt. 1978.
4. Noakowski, P.: "Practicable Method for the Design of Circular Reinforcement of Industrial Chimneys", Fourth International Symposium on Industrial Chimneys, The Hague,11 and 12 May, 1981.
5. Noakowski, P.: "Mitwirkungsgesetze zur Ermittlung der Verformungen und der Zwangbeanspruchung bei gleichzeitiger Lastbeanspruchung"; Beton- und Stahlbetonbau 81 (1986), pages 318-325.
6. Noakowski, P.:"Verbundorientierte, kontinuierliche Theorie zur Ermittlung der Rißbreite" or "Continuous theory for the determination of crack width under the consideration of bond" (in German and English),Beton- und Stahlbetonbau 80 (1985).
7. Noakowski, P., Schafer, H.G.,: "Control of crack width: comparison of predictions in CICIND and EC2", University of Dortmund, Germany,1998.
8. England,G.,Phillips,E.: "Effect of Shrinkage and Creep on the Short- and Long-term State of Stress in Reinforced Concrete Chimneys"; Chimney Design Symposium, Edinburgh, April 1973.
9. Krichevsky,A.P.,Brizhaty,O.E.,Korsun,V.I. & Krichevsky.S.A., "Temperature effects in Reinforced Concrete Chimneys and the prospects of Steel Fibre Shotcrete for Reinforcement of Concrete Chimneys"; CICIND Report Vol.12, No.1,1996.

$$-n_u = -\frac{-N_u}{t\, f_{ck}}$$

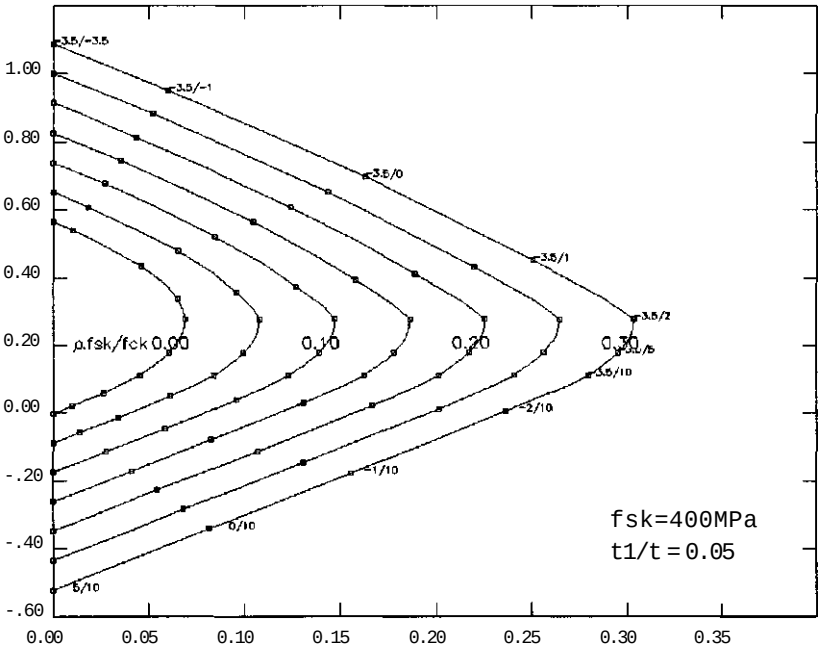

$$m_u = \frac{M_u}{t^2 f_{ck}}$$

Fig. 7: Dimensioning Diagram for the Determination of the Ratio of Reinforcement $_p$ and the Wall Thickness t of Rectangular Cross-sections with $t_1/t = 0.05$

$$-n_u = -\frac{-N_u}{t\, f_{ck}}$$

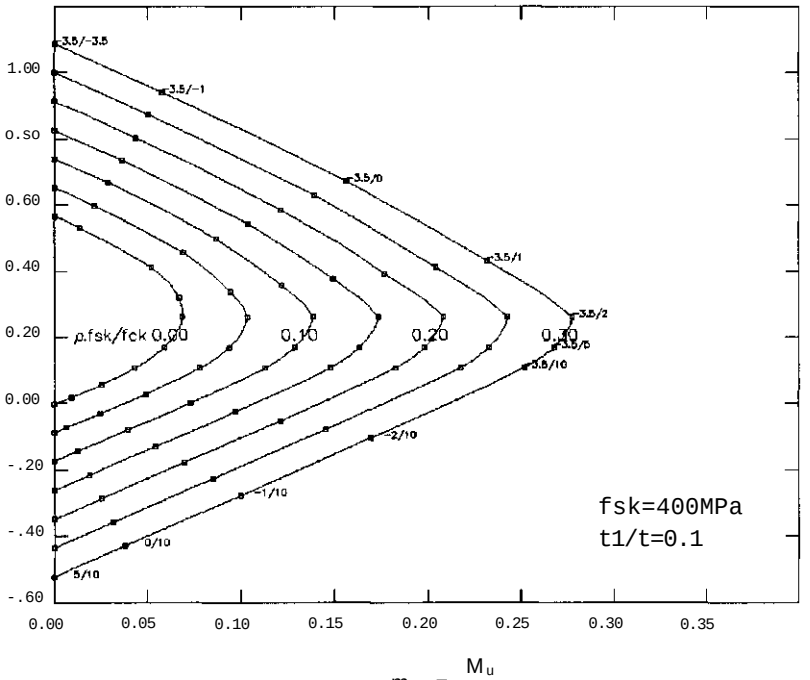

$$m_u = \frac{M_u}{t^2 f_{ck}}$$

Fig. 8: Dimensioning Diagram for the Determination of the Ratio of Reinforcement p and the Wall Thickness t of Rectangular Cross-sections with $t_1/t = 0.10$

$$-n_u = -\frac{-N_u}{t\, f_{ck}}$$

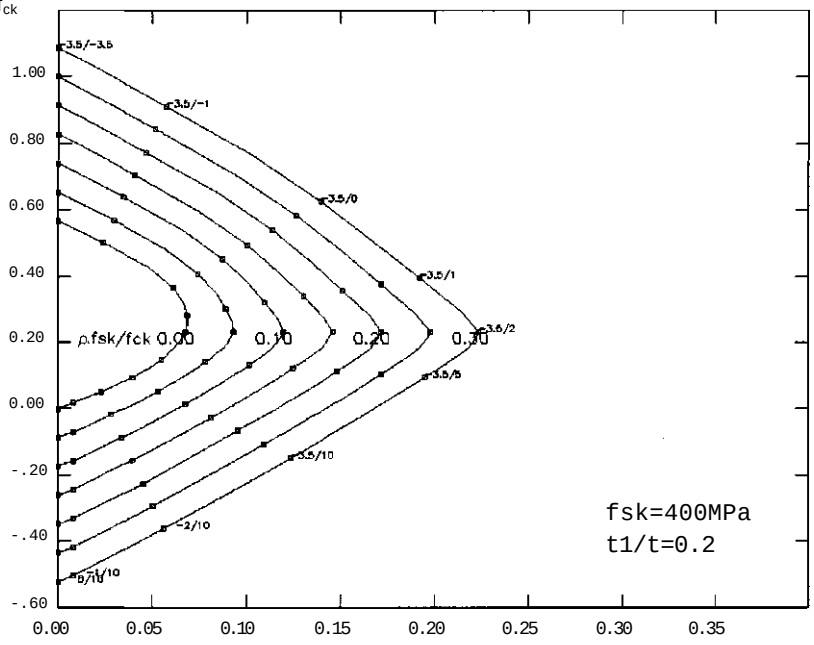

$$m_u = \frac{M_u}{t^2 f_{ck}}$$

Fig. 9: Dimensioning Diagram for the Determination of the Ratio of Reinforcement p and the Wall Thickness t of Rectangular Cross-sections with $t_1/t = 0.20$

Commentary No. 8

Seismic Actions

Table of Contents

1 General

1.1 Overview

This commentary extends section 7.3 of the Model Code to provide a more detailed description of the calculation of the actions.

2 Elastic response

2.1 Typical design response spectrum

The seismic action is described by means of a standardised acceleration response spectrum. The spectrum is given as a function of the period (T) of the structure by the expressions (1) and plotted ir Figure 1:

$$\begin{aligned} &\text{for} \quad T \le 0.1s: && a_s(T) = a(1 + 20T) \\ &\text{for} \quad 0.1s < T \le 0.4s: && a_s(T) = 3a \\ &\text{for} \quad 0.4s < T: && a_s(T) = 3aS(T/0.4)^{\beta} \le 3a \end{aligned} \qquad (1)$$

where

- **T** period of the structure in seconds
- **a** maximum effective peak ground acceleration at the location of the chimney
- **S** Soil factor depending on soil type, see Table 3
- **β** Soil exponent, see Table 3

2.2 The Effect of Weak Soil Layers

The presence of soil overlying rock modifies the amplitude and frequency content of the earthquake ground motion. Figure 1 presents normalised response spectra for three types of soil designated S1, S2 and S3. The curve S=1 is applicable for stiff soils or soil with rock at a depth of 0 to 10 m. The curve with S = 1.2 holds for soft or medium stiff soils over rock at a depth between 10 and 60 m whilst the curve with S = 1.5 holds for soft or medium stiff soils of depth greater than 60 m. The classification of soil as soft or medium stiff depends on the relative density for non-cohesive soils and on the sensitivity ratio for cohesive soils.

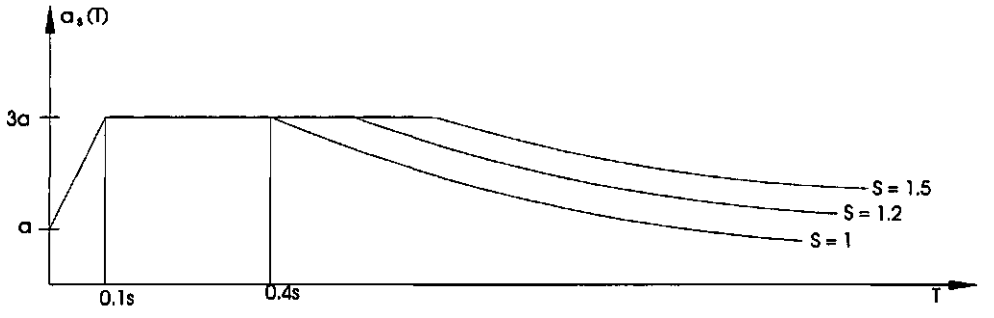

Figure 1 Response spectra for different soil types

The Relative Density is a measure of the voids in the soil and can only be determined for soils with a low fines content The Sensitivity is the ratio between the shear strength of a specimen in the undisturbed state and its shear strength after remoulding. This ratio can only be used for cohesive soils. The values of Relative Density and Sensitivity are given in Table 2.

Representative normalised design response spectra for different soil sites are also presented in the 1997 "Uniform Building Code" of the USA [6] and the European standard "Eurocode 8:design provisions for the earthquake resistance of structures" [7].

Table 1: Determination of Soil Type from Soil Condition and Soil Depth

Soil Depth to Rock(m)	Soil Condition	
	Stiff	Soft or Medium Stiff
0to10	S1	S1
10 to 60	S1	S2
>60	S1	S3

The classification of soil condition as stiff, medium stiff or soft follows from Table 2.

Table 2: Classification of Soil Condition according to Soil Characteristic

Soil Characteristic		Soil Condition
Non-Cohesive Soil:	Cohesive Soil:	
Value of Relative Density	Value of Sensitivity	
<0.3	<8	stiff
0.3 to 0.8	8 to 30	medium
>0.8	>30	soft
The Relative Density is a measure of the deposition condition in the soil. The Sensitivity is the ratio between the undrained shear strength of a specimen in undisturbed and remoulded states.		

For piled foundations, the soil type is determined according to the condition at the toe of the piles.

Table 3: Soil Factor S and Soil Exponent β for the Three Soil Types

Soil Type	Soil Factor S	Soil Exponent β
S1	1.0	-0.8
S2	1.2	-0.67
S3	1.5	-0.67

2.3 Peak ground acceleration

If the intensity of ground motion is defined by the Modified Mercalli Scale I_{MM}, the peak ground acceleration a can be determined from Table 4.

Table 4: Peak ground acceleration as a function of Modified Mercalli Scale I_{MM}

'MM	a
VI	0.07g
VII	0.15g
VIII	0.30g
IX	0.50g
X	0.70g
g is the acceleration due to gravity	

The maximum response in each mode does not occur simultaneously since the modes are not exactly in phase. Consequently the overall response of the chimney is calculated using a root sum square method to combine the individual modal contributions. The theory associated with the response spectrum method is presented in many earthquake engineering reference books such as [1].

2.4 Response spectrum method

Initially the mode shapes and the associated normalised deflections $\bar{u}_i$, shear forces $\bar{Q}_i$ and moments $\bar{M}_i$ are calculated by modal analysis. The response of the chimney in each mode Ui is estimated using the equation:

$$u_i = \bar{u}_i N_i$$

where

$$N_i = \frac{P_i T_i^2}{4\pi^2} a_s(T_i)$$ N_i = Modal scaling factor

$$P_i = \frac{\int_0^h \bar{u}_i(z)m(z)dz}{\int_0^h \bar{u}_i^2(z)m(z)dz}$$ P_i = Modal participation factor

The scaling factor N_i used for the mode shape u_i will also apply for the moments and shear forces.

2.5 Modulus of Elasticity

Increasing the stiffness of the chimney increases the resonant frequencies and increases the earthquake induced loads. Therefore the short-term values for the modulus of elasticity given by equation (8.3) of the Model Code should be used in calculating the frequencies of the various modes.

2.6 Second Order Effects

The effects of second order moments developed under earthquake excitation are considered negligible and may be neglected.

2.7 A World Map of Earthquake Areas

Figure 2 (from [2]) is presented as a separate sheet at the back of the Commentaries and presents as a guide a world map of seismic hazards including an estimate of seismic risk in terms of the risk of exceedence of different levels of peak ground acceleration. The relation between the Mercalli scale and the peak acceleration given in Table 4 is a simplification of empirical values. It is recommended that site specific acceleration values be determined and used for design purposes.

3 Seismic Design Actions

The seismic design actions are obtained from the elastic response by multiplying the actions by an importance factor (IF) and dividing by a structural response factor (R).

3.1 Importance factor

The importance factor is dependent on the importance class of the chimney:

Class 1: IF = 1.2(R=1)orIF = 1.0(R=2)

Class 2: IF = 1.4

3.2 Structural response factor

The structural response factor is dependent on the level of seismic detailing:

R = 1 No specific seismic detailing

R = 2 Seismic detailing in accordance with Section 7.3.4.3 of the Code (this implies the use of Capacity Design)

3.3 Return periods

The importance factors and structural response factors have been selected so that the return periods associated with the serviceability limit state and the structural stability limit state are reasonable. The serviceability limit state (SLS) is associated with the ultimate strength of the chimney being reached whilst the structural stability limit state (SSLS) is associated with inelastic failure of the chimney. Based on analytical studies the ratio of ground acceleration between the SSLS and SLS has been assumed equal to 1.4 and 1.4 x 4 = 5.6 for the non-seismic and seismic designs respectively, where the factor 1.4 reflects the available flexural overstrength . The design basis (DB) earthquake is associated with a return period of 475 years.

The effective return periods are listed in the following table for each of the different chimney classes, levels of detailing and levels of seismicity. The table also lists the ratios of the acceleration coefficients (peak effective ground accelerations) associated with the SLS (a_e/a_{475}) and SSLS (a_f/a_{475}) events to the DB event.

Class	Detailing	Seismicity	IF	R	a_f/a_e	a_e/a_{475}	a_f/a_{475}	Return Period (Years)		
								DB	SLS	SSLS
1	Elastic	Low	1.2	1	1.4	1.2	1.7	475	730	1750
		High	1.2	1	1.4	1.2	1.7	475	1130	7700
1	Seismic	Low	1.0	2	5.6	0.5	2.8	475	120	8300
		High	1.0	2	5.6	0.5	2.8	475	40	10000+
2	Elastic	Low	1.4	1	1.4	1.4	2.0	475	1075	2700
		High	1.4	1	1.4	1.4	2.0	475	2600	10000+
2	Seismic	Low	1.4	2	5.6	0.7	3.9	475	220	10000+
		High	1.4	2	5.6	0.7	3.9	475	120	10000+

Table 5 - Return periods associated with different limit states

The return periods of different earthquake events have been calculated on the basis of a generic seismic hazard map (Figure 1) and the following approximate relationship [4],[5] between effective peak ground acceleration (ay) and return period (T).

$$a_T = \left[\frac{1}{\beta}\mathrm{Ln}(T)\right]^{(1/N)}$$

where p, N are seismicity dependent and summarised in Table 6.

(It should be emphasised that the prediction of return periods for a given level of seismicity is an inexact science and the values should be taken as indicative and approximate only. Recent paleoseismic studies have suggested that the peak ground acceleration associated with long return period events in regions of low seismicity may be higher than indicated in Figure 3 [8].)

Parameter	Seismicity			
	Very Low	Low	Moderate	High
β	17.3	14.2	12.3	12.3
N	0.36	0.37	0.42	0.72
$^{a}_{500}$	0.05g	0.10g	0.20g	0.40g

Table 6 - Seismicity parameters

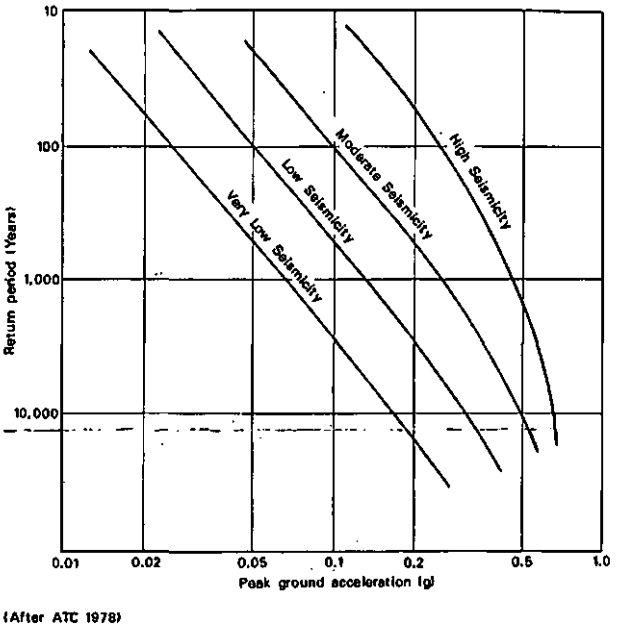

Figure 3 - Peak ground acceleration as a function of return period and seismicity

4 References

1) Wiegel, R. L: Earthquake Engineering, 1970, Prentice Hall, Englewood Cliffs, New York.

2) GSHAP Map, from a UN/IDNDR Program carried out by the International Lithosphere Program, 1999.

3) Wilson, J.L., 2000,"Code recommendations for the aseismic design of tall reinforced concrete chimneys", CICIND Report Vol.16 No.2.

4) Applied Technology Council, 1978, "ATC 3-06" Tentative provisions for the development of seismic regulations for buildings", USA.

5) Booth, E., 1984, "Assessment of Seismic Hazard", Arup Journal, June pp 13-21.

6) UBC,1997,"Uniform Building Code" International Conference of Building Officials, Whittier, California, USA.

7) CEN,1996,"Eurocode 8:Design provisions for earthquake resistance of structures" Draft ENV 1996-1.

8) FEMA, 1997, "NEHRP guidelines and commentary for the seismic rehabilitation of buildings: FEMA 273" Federal Emergency Management Agency, Washington DC,USA.

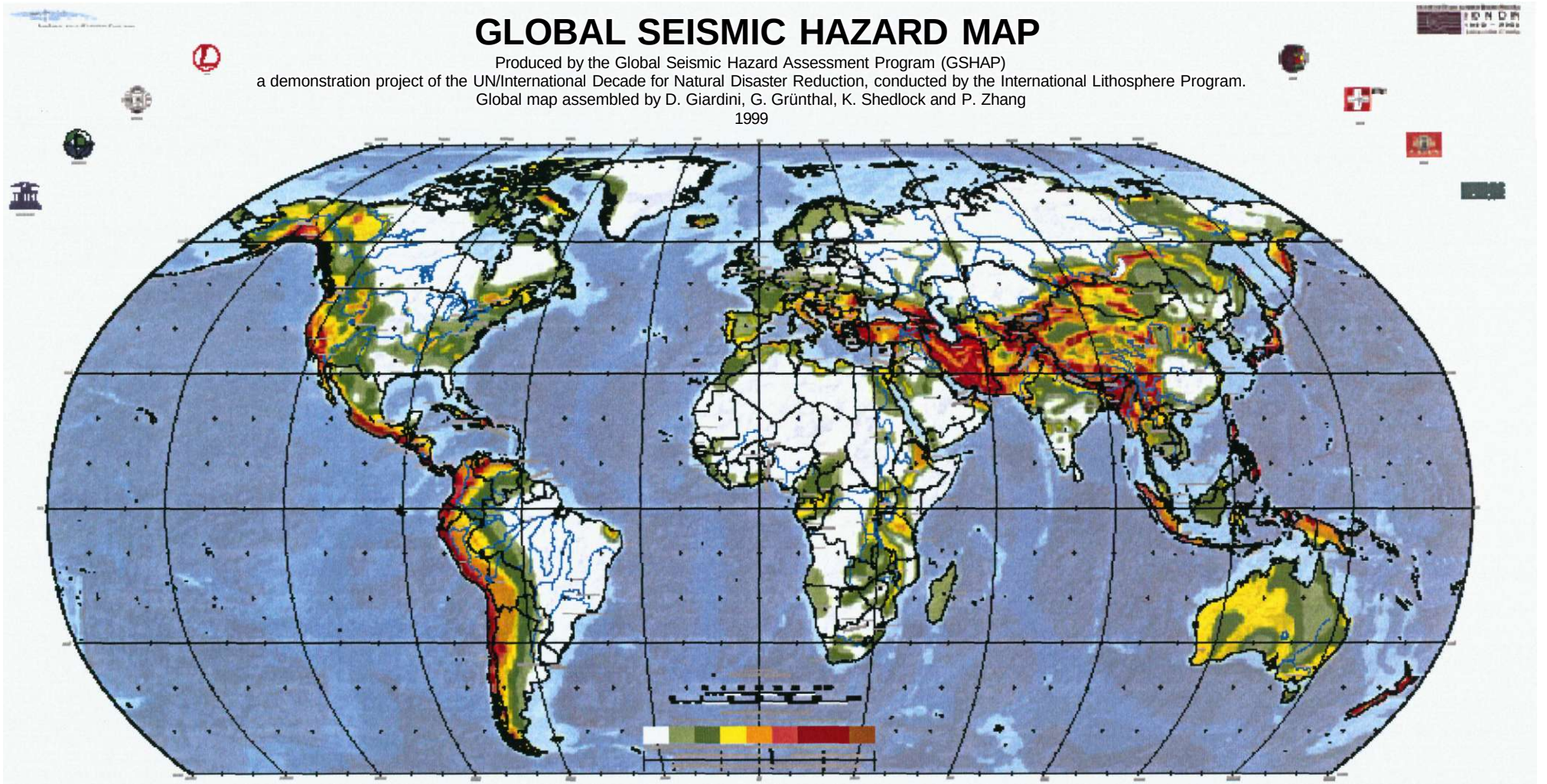

Figure 2 Global Seismic Hazard Map
(from GSHAP programme for the UN IDNDR project)